

**INVESTIGATIVE STUDY OF RADIOTOXICITY OF SPENT NUCLEAR FUEL  
ASSEMBLY OF SOME COMMERCIAL NUCLEAR POWER PLANTS**

**CASE STUDY: *EUROPEAN PRESSURIZED WATER REACTOR AND HUALONG  
ONE PRESSURIZED WATER REACTOR***

BY

**OJO, OLANREWaju PETER  
(10633006)**

This Thesis is submitted to the Department of Nuclear Engineering,  
School of Nuclear and Allied Sciences, University of Ghana, Legon

In partial fulfillment of the requirement for the award of

**Master of Philosophy Degree**

**in**

**Nuclear Science and Technology**

July, 2018

**DECLARATION**

I hereby declare that, this thesis is the undertaken of OJO OLANREWAJU PETER under the supervision of Dr. ROBERT BRIGHT MAWUKO SOGBADJI and Dr. REX GYEABOUR ABREFAH both of the School of Nuclear and Allied Sciences (SNAS), University of Ghana (UG).

.....

OJO OLANREWAJU PETER

DATE: .....

.....

DR. ROBERT B. M. SOGBADJI  
(Principal Supervisor)

DATE: .....

.....

DR. REX G. ABREFAH  
(Co-Supervisor)

DATE: .....

## ABSTRACT

The European Pressurized Water Reactor (EPR) and Hualong One Pressurized Water Reactor (HPR) are two of the reactors under consideration by the Ghana Nuclear Power Programme. Radiotoxicity analysis of Spent Nuclear Fuel (SNF) assembly was carried out with these commercial Pressurized Water Reactor (PWR) nuclear power technology as case study. Burnup depletion calculation for the Uranium Oxide (UOX) fuel of these reactor technologies was simulated. Monte Carlo Neutron Particle Extended (MCNPX), a code used in nuclear fuel management analysis, was chosen in this study for the Burnup depletion calculation, being a well validated code and due to its versatile nuclei reactions cross section library.

Determination of radiotoxicity for EPR and HPR SNF is the main objective of this study. The radiotoxicity was achieved taking into consideration the radioactive decay rate of the radionuclides and the Dose Factor of each radionuclide present in the SNF using the International Commission on Radiological Protection (ICRP) compendium of Dose Factors due to ingestion. The radiotoxicity for the two reactor's SNF were compared. The initial radiotoxicity for HPR SNF was higher in the duration below one hundred years but at about a hundred years and above, the radiotoxicity was higher for EPR SNF. The radiotoxicity was tremendously reduced for the reprocessed spent UOX fuel (with the Pu and U extracted) to be used as mixed oxide (MOX) fuel. The main finding is that Pu isotopes are the major contributors to the radiotoxicity of the SNF for the two reactors systems due to their very high radioactivity, long half-lives and high dose factors as compared to other actinides and fission products present in the SNF.

## **DEDICATION**

This research work is dedicated to my parents Mr Sunday Ojo and Mrs Modupe Ojo. Dedicated also to my fiancée, Deborah Babatunde, my brothers, Ayo Ojo, Femi Ojo and to all my friends.

## ACKNOWLEDGEMENT

Foremost, I give thanks to Almighty God for the strength He gave me and for keeping me in good health throughout the period of undertaking this study. I thank the International Atomic Energy Agency (IAEA) and the Government of Nigeria and my Director General, Prof. Mallam for giving me the opportunity to undertake this Master program.

I reiterate my utmost gratitude to Dr. R.B.M Sogbadji and Dr. Abrefah, for their understanding, encouragement and personal guidance.

Many thanks to the staffs of Nigeria Atomic Energy Commission for their support. I thank Dr. Agedah and Dr. Ofodile for their support.

Lastly, my deep gratitude goes to my parents, friends, colleagues and lecturers of School of Nuclear and Allied Sciences for their love and support, also for their incessant prayers and encouragement through the years I've been studying and during the period of this study. It would have been impossible to achieve this accomplishment without them. I thank you all so much.

**TABLE OF CONTENTS**

DECLARATION .....	i
ABSTRACT.....	ii
DEDICATION.....	iii
TABLE OF CONTENT.....	v
ACKNOWLEDGEMENT .....	iv
LIST OF TABLES.....	viii
LIST OF FIGURES .....	ix
LIST OF ABBREVIATION AND SYMBOLS .....	x
CHAPTER ONE.....	1
1 Introduction.....	1
1.1 Background of The Study.....	1
1.2 Statement of Research Problem and Justification of Study.....	5
1.2.1 Overview of The Pressurized Water Reactor Designs.....	6
1.2.1.1 European Power Reactors (EPR).....	8
1.2.1.2 EPR Design Overview .....	8
1.2.1.4 Design Overview of the HPR-1000 .....	12
1.3. Objectives .....	15
1.3.1 Main.....	15
1.3.2 Specifics.....	15
1.4. Scope of Study.....	15
1.5. Organisation of the Research.....	15
CHAPTER TWO.....	17
2.0 Literature Review.....	17
2.1 General.....	17
2.2 Previous Related Works.....	17
2.2.1 MCNPX.....	17
2.2.2 Radiotoxicity.....	22
CHAPTER THREE .....	33
3.0 THEORETICAL ANALYSIS .....	33
3.1 Introduction.....	33
3.2 Nuclear Reactor Theory.....	33
3.3 Neutron Transport Theory .....	34
3.4 Methods Used to Solve or Simulate Neutron Transport.....	36

3.4.1 Deterministic Methods.....	36
3.4.2 Stochastic Methods (Monte Carlo Method).....	37
3.5 Isotopic Depletion.....	38
3.6 CINDER'90 .....	40
3.6.1 CINDER Atom Density Algorithm (Markovian Chains) .....	40
3.7 MCNPX/CINDER'90.....	43
3.8 Radiotoxicity.....	46
CHAPTER FOUR.....	49
4.0 METHODOLOGY .....	49
4.1 Introduction.....	49
4.2 MCNPX .....	49
4.3 MCNPX Model of the Reactors.....	50
4.3.1 HPR and EPR Models.....	50
4.4 Source Parameters.....	53
4.4 Material Specification.....	54
4.5 Burn Card Setup.....	54
4.6 Radiotoxicity.....	57
CHAPTER FIVE .....	58
5.0 RESULTS AND DISCUSSION.....	58
5.1 Introduction.....	58
5.2 Nuclear Fuel Reactivity .....	59
5.3 The Effective Multiplication Factor .....	59
5.4 Burnup .....	61
5.5 Time Evolution of the Major actinides in the EPR and HPR UOX fuel .....	62
5.6 Radiotoxicity.....	65
5.6.1 Radiotoxicity due to the Actinides and Fission product in the SNF.....	65
5.6.2 Radiotoxicity by Ingestion from Actinides.....	67
5.6.3 Plutonium isotopes Impact on the Ingestion Radiotoxicity .....	71
5.6.4 Fission Products Impact on Radiotoxicity .....	73
5.6.5 Comparison of the Ingestion Radiotoxicity with and without Pu and U .....	76
5.6.6 Ingestion Radiotoxicity comparison for the EPR and HPR SNF .....	78
CHAPTER SIX.....	81
6.0 Conclusion and Recommendation .....	81
6.1 Conclusion .....	81

6.2 Recommendation .....	82
References.....	84

**LIST OF TABLES**

Table 4. 1 Fuel Assemblies Design Specifications ..... 51

**LIST OF FIGURES**

Figure 1. 1 EPR Plant layout..... 9

Figure 1. 2 EPR Reactor Pressure Vessel ..... 10

Figure 1. 3 HPR plant layout ..... 13

Figure 2. 1 Result showing Atom density of various actinides as a function of Effective full power days. (Boafo, Alhassan, & Akaho, 2014)..... 20

Figure 2. 2 Sogbadji, et al 2016., Result of Radiotoxicity Calculation for UOX fuel of French EPR at burnup of 46GWd/t..... 24

Figure3. 1 MCNPX & CINDER'90 Predictor Corrector Method..... 45

Figure 4. 1 MCNPX Plot of Transverse Section of HPR Fuel Pin ..... 52

Figure 4. 2 MCNPX Plot of Longitudinal Section of the EPR and HPR Fuel Pin Respectively..... 52

Figure 4. 3 MCNPX Plot of Transverse Section HPR Fuel Assembly..... 53

Figure 5. 1  $k_{eff}$  Values against Burnup Time for EPR and HPR..... 60

Figure 5. 2 EPR and HPR Burnup Profile ..... 61

Figure 5. 3 Atom density of the major Actinides with burnup time EPR..... 62

Figure 5. 4 Atom density of the major Actinides with burnup time HPR ..... 63

Figure 5. 5 U-238 atom densities for EPR and HPR ..... 64

Figure 5. 6 Ingestion Radiotoxicity from Fission Product and Actinide in EPR SNF ..... 66

Figure 5. 7 Ingestion Radiotoxicity from Fission Product & Actinide in HPR SNF..... 67

Figure 5. 8 Ingestion Radiotoxicity by Actinides in EPR SNF ..... 68

Figure 5. 9 Radiotoxicity by Ingestion from Actinides in HPR SNF ..... 69

Figure 5. 10 Impact of Pu Isotopes on Radiotoxicity of EPR SNF ..... 71

Figure 5. 11 Impact of Pu Isotopes on Radiotoxicity of HPR SNF ..... 72

Figure 5. 12 Radiotoxicity by Ingestion from Fission Products in EPR SNF ..... 75

Figure 5. 13 Radiotoxicity by Ingestion from Fission Products in HPR ..... 76

Figure 5. 14 Radiotoxicity by Ingestion without Pu and Am Isotopes for EPR SNF..... 77

Figure 5. 15 Radiotoxicity by Ingestion without Pu and U Isotopes for HPR SNF ..... 78

Figure 5. 16 Comparison of Radiotoxicity by Ingestion For EPR and HPR SNF ..... 79

**LIST OF ABBREVIATION AND SYMBOL**

$\%$	Percent
$^{\circ}C$	Degree Celsius
$A(Bq)$	Activity in Bequerel
$Ac$	Actinium Nuclei
$ADS$	Accelerator Driven System
$AFMIN$	Atomic fraction Minimum
$Am$	Americium Nuclei
$APSI$	Atomic Power Station 1
$Ba$	Barium Nuclei
$BOPT$	Burnup Option
$Bq$	Bequerel
$CF$	China Fuel
$Cm$	Curium Nuclei
$DCF$	Dose Conversion Factor
$EBR$	Experimental Breeder Reactor EBR
$ENDF$	Evaluated Nuclear Data File
$EOC$	End Of Fuel Cycle
$EPR$	French European Pressurised Water Reactor
$FA$	Fuel Assembly
$FP$	Fission Product
$GWd/MtU$	GigaWatt day per Metric tonne of Uranium
$h_{E,50}$	The committed effective dose equivalent per unit intake of radionuclide

$h_{T,50}$	The tissue dose equivalent conversion factor for organ or tissue T (expressed in Sv/Bq), i.e., the committed equivalent dose per intake of radionuclide
<i>HEU</i>	Highly Enriched Uranium
<i>HLW</i>	High Level Waste
<i>HPRI000</i>	Chinese Hualong one Pressurised Water Reactor
<i>I</i>	Iodine Nuclei
<i>ICE</i>	Isotope Correlation Experiment
<i>ICRP</i>	International Commission on Radiological Protection
<i>IMC</i>	Inert Matrix Combined
<i>KCODE</i>	Criticality Code
$K_{eff}$	Effective Multiplication factor
<i>LEU</i>	Low Enriched Uranium
<i>LOCA</i>	Loss of Coolant Accident
<i>LWR</i>	Light Water Reactor
<i>MA</i>	Minor Actinides
<i>MAT</i>	Material
<i>MCNPX</i>	Monte Carlo Neutron Particle Extended
<i>MNSR</i>	Miniature Neutron Source Reactor
<i>MOX</i>	Mixed Oxide
<i>MPa</i>	MegaPascal
<i>MWd/kg</i>	Megawatt day per Kilogram
<i>MWe</i>	Megawatt Electric
<i>MWt</i>	Megawatt thermal
<i>n</i>	Neutron
<i>Np</i>	Neptunium Nuclei

<i>NPI</i>	Nuclear Power International
<i>NPP</i>	Nuclear Power Plants
<i>P&amp;T</i>	Partitioning and Transmutation
<i>Pa</i>	Protactinium Nuclei
<i>PFRAC</i>	Power Fraction
<i>Pu</i>	Plutonium Nuclei
<i>PWR</i>	Pressurised water Reactor
<i>R(Sv)</i>	Radiotoxicity in Siervert
<i>RCCA</i>	Rod Cluster Control Assembly
<i>RCP</i>	Reactor Coolant Pump
<i>RCS</i>	Reactor Cooling System
<i>RPV</i>	Reactor Pressure Vessel
<i>Ru</i>	Ruthenium Nuclei
<i>SDEF</i>	Source Definition
<i>SNF</i>	Spent Nuclear Fuel
<i>Sr</i>	Strontium Nuclei
<i>Tc</i>	Technetium Nuclei
<i>Th</i>	Thorium Nuclei
<i>U</i>	Uranium Nuclei
<i>UOX</i>	Uranium Oxide
<i>VHTR</i>	Very High Temperature Reactor
<i>VVER</i>	Vodo-Vodyanoi Energetichesky Reaktor
$W_T$	The Weighing Factor for the Tissue
<i>Xe</i>	Xenon Nuclei
<i>XSDIR</i> Cross-section Directory	

$\beta$	Beta particle
$\gamma$	Gamma ray
$\rho$	Reactivity
$\Phi$	Neutron flux
$Sv$	Sielvert
$\sigma$	Cross Section for Thermal Neutron

## CHAPTER ONE

### 1 Introduction

In this chapter, the background of the study is presented and also the basis for conducting the research. The chapter also provides information on problem statement, relevance and justification of the research, objectives and scope of the research, and concludes with an elaboration of the structure of the study.

#### 1.1 Background of The Study

In the year 1951, December 20th to be precise, for the very first time in history, nuclear energy was used to produce electricity capable of lighting four bulbs at the Experimental Breeder Reactor EBR1 in Idaho, United States of America. However, this was only experimental to confirm the breeder reactor idea. The very first Nuclear Power Plant that was connected to the power grid was the APS1 capable of 5MW electrical output. It was built at Obninsk in Russia and connected to the power grid on June 26, 1954. The very first commercial nuclear power plant was built in England. Calder Hall 1 as it is known, was connected to the power grid on August 27th, 1956. It was capable of 50MW electricity (European Nuclear Society, 2017).

According to statistics, as of November 28th 2016, in 31 countries worldwide, 450 nuclear power plants operates with net electric capacity of about 392 GW and 60 plants with an installed capacity of 60 GW are under construction in 16 countries (European Nuclear Society, 2017).

The only commercial nuclear power plant in Africa is in South Africa (wikipedia, the free encyclopedia, 2018).

South Africa boasts of two reactors located at the Koeberg nuclear power station, which produces about 5% of South Africa's electricity. Other countries in Africa have also shown interest in utilizing nuclear energy for electricity generation.

Ghana as a country has made efforts towards adding nuclear power to the energy mix. The government took a serious look at the nuclear option in 2007 during the occurrence of the third energy crisis. There was a deficit of about 400MW in power supply from the hydro system. The import bill of crude oil climbed due to high price on the international market and the erratic supply through the west Africa gas pipeline. The President in May 2007 therefore set up an eight-member committee to advise government on the potential use of nuclear energy for electricity generation to develop a roadmap, which must conclude a pre-feasibility study. After its valuation, the committee concluded that since nuclear energy is an established technology, which has witnessed significant improvements in economic performance and operational safety in recent years, it is capable of providing safe, reliable and economically modest electricity with very low carbon emissions. A roadmap was developed, which proposed the formation of Presidential Commission on Nuclear Power Development and a 400 MW nuclear power plant to start commercial operation in 2018. A Cabinet decision was taken in early 2008 to proceed with the roadmap. (www.modernghana.com, 2008).

As part of the preparations being made towards the implementation of the nuclear power project, detailed assessment on the type of reactor considered was made based on the following criteria ; economics, technological maturity, suitability to the Ghanaian and West African grid size, passive safety and standardization of design. The results obtained

showed that a 300MW to 700MW capacity pressurised water reactor will suffice. (Ennison & Dzobo, 2018).

However, there are associated risks in utilising nuclear energy for energy generation just like any other natural resources for energy production. The argument most commonly brought up by the challengers of the application of nuclear energy is the long-term risk caused by the long-lived isotopes that can be found in the spent nuclear fuel of Nuclear Power Plants (NPPs). There are significant differences between these risks depending on the type of the nuclear energy system.

Ever since the development of nuclear energy for power generation, there have been the problem of dealing with the long-lived radioactive waste generated from the operation of nuclear power plants. Construction of long-term controllable storage facility is typical in addressing this menace. Other approach has been to transmute such wastes to reduce their half lives.

Recent researches (Csom, Feher, & Szieberth, 2001) has shown the efficacy of partitioning and transmutation (P&T) technology to decrease the required storage time by several orders of magnitude.

However, in order to choose the best P&T strategy circumspect evaluations should be performed, and these evaluations should be based on the analysis of long-term risk.

For correct choice of strategy of a long-term storage of spent nuclear fuel, information on how the radioactive waste's major characteristics vary with time during long-term storage is important (Csom, Feher, & Szieberth, 2001). Pieces of Informations like its radioactivity level is vital ; this will help in determining the radiotoxicity.

These characteristics will depend on the operational characteristics of the nuclear fuel.

These include :

1. Initial enrichment : this impacts potential final burnup. The more the fissile content the more the burnup.
2. Irradiation history : this is a record of the specific power or energy released from the nuclear fuel as a function of time.
3. Burn-up : The overall energy released in fission by a certain amount of nuclear fuel is referred to as its burnup. It is measured in megawatt days per metric tonne of uranium (MWd/MTU). It is the integral of irradiation history curve.
4. Cooling time : i.e the amount of time after the final irradiation of the spent fuel assembly for cooling before storage.

Spent nuclear fuel (SNF) is nuclear fuel that has been irradiated by neutrons in a nuclear reactor. It is no more helpful in supporting a nuclear response in a reactor and based on its point along the fuel cycle, it might have significantly varying isotopic constituents (wikipedia, 2018). These isotopic constituents include the fission products, activation products and the actinides which constitutes the radioactivity and hence the radiotoxicity of spent nuclear fuel.

Radiotoxicity is the quantity most widely used to describe the long-term risk of radioactive wastes (Csom, Feher, & Szieberth, 2001).

The simplest definition of radiotoxicity refers to the activity concentration of the stored waste (Csom, Feher, & Szieberth, 2001). A different concept of radiotoxicity can also be defined as the expected radiation dose in case of a release from the storage (Csom, Feher, & Szieberth, 2001). The radiotoxicity of radionuclide could vary depending on whether

it is inhaled in the air or ingested through food or water. It is influenced by the energy of its radiation, the tissue that absorbs it in the organism and how long it stays in the body.

(Csom, Feher, & Szieberth, 2001)

Radiotoxicity of spent nuclear fuel originates from alpha decay and beta decay of its fission products and actinides. When fissile U-235 absorbs a neutron, it splits into fission products. These fission products have high fission absorption coefficient and thus reduces the neutron density, causing a deficit in neutron population required to sustain a chain reaction, so the fuel is said to be spent, even when the fuel is not yet burned up.

Actinides on the other hand are produced from neutron capture processes in the fuel to produce high mass elements with very long half-life and decay slowly to release large amounts of energy mainly from alpha decay.

## **1.2 Statement of Research Problem and Justification of Study**

In view of the anticipated risk associated with utilizing nuclear technology for power, Ghana will have to evaluate and analyse some of the existing candidate technologies to ascertain which technology is safer based on the radiotoxic analysis of the spent fuel assembly of the nuclear technology considered, to ensure safety of the environment.

This study is concentrated on the radiotoxicity analysis of spent fuel assembly of some commercial Nuclear Power Plants (pressurized water reactors) under consideration by the Ghana Nuclear Power Program. In this study, two were studied, namely;

- the Chinese Hualong one Pressurised Water Reactor HPR1000,
- the French European Pressurised Reactor EPR.

Ghana's position to move for nuclear power has made Radiotoxicity analysis (which reflect to what extent the radioactive decays could jeopardize the biosphere), a necessity.

This study can help in making a choice on the nuclear fuel cycle to adopt and in fuel characterization and disposal (fuel management). It can also be applied in emergency preparedness and response. The next section gives an overview of the reactors considered.

### **1.2.1 Overview of The Pressurized Water Reactor Designs**

Currently, the most common type of commercial nuclear power reactors is the pressurized water reactor, known by its abbreviation PWR. The first PWR reactors were intended for military ship propulsion by the Westinghouse Bettis Atomic Power Laboratory and then commercialized by the Westinghouse Nuclear Power Division. The 60MWe Shipping-port located in Pittsburgh, Pennsylvania in the United States was the first of its kind commercial PWR.

The PWR consists of two main systems ; a primary (reactor) system and a secondary (steam) system. This is to restrain the radioactive materials to the reactor system. In the primary loop, heat is generated from the controlled fission reaction into the coolant at a pressure of about 15.5 MPa so that it circulates within the primary loop at a high temperature of 325 °C without boiling. At the steam generator, heat is removed from the coolant (primary loop) into the secondary loop where steam is generated. The coolant is then pumped back in a repeated cycle. A pressurizer is connected to keep the pressure above saturation pressure to prevent bulk boiling in the reactor system (in Bulk boiling, the temperature of the liquid slightly exceeds the saturation temperature). In the secondary loop, the steam produced in the steam generator is pumped to a turbine which drives a

generator to produce electrical energy. The steam is then condensed and pumped back into the steam generator in a repeated manner.

The reactor vessel houses the core cask, the heat-generating core, coolant circulating channels and associated supports and controls. The PWR has a cylindrical shaped reactor vessel with hemispherical heads at the top and bottom. The upper head is removable to allow for refueling of the reactor. The coolant loop of the reactor system has an inlet nozzle at the “cold leg” and an outlet nozzle at the “hot leg”. The fuel is surrounded by the core cask fitted inside the reactor vessel. It creates an annular channel to enhance coolant flow and also protects the vessel by lessening some of the radiations emanating from the radioactive fuel. The fuel assembly sits on the lower core supporting plate at the bottom of the core cask.

The PWR core consists of 150 to 200 fuel assemblies arranged in a square lattice. Typically, a PWR fuel assembly has between 200 and 300 fuel rods arranged in a 15 x 15 to 17 x 17 square array. Within the fuel assemblies are control rods which are incorporated into the assembly by control guide tubes which replace up to a third of the fuel rods. Other rods within the assemblies contain no fuel and are filled instead by instrumentations and burnable poisons such as boron to extend the core life. The fuel is made of pellets with enrichment between 2.1 to 3.5% in U-235. These pellets are 0.813 cm in diameter and 1.53 cm in length. The pellets are pressed and enclosed in a Zircalloy-4 cladding tube with a wall thickness of about 0.064 cm. Zircalloy has a very good mechanical strength and more importantly, a low neutron absorption cross-section helping the neutron economy in the PWR.

Light water is used as both the coolant and the moderator in all PWR designs. The water enters the core at a temperature of about 257<sup>0</sup>C via the lowest part. The water is heated as it flows through the reactor core and exit the core at a temperature of about 315<sup>0</sup>C. Like all other thermal reactors, the PWR requires that fast fission neutrons are thermalized in order to interact with the fissile U-235 in the nuclear fuel to sustain the nuclear chain reaction. This thermalization process is achieved through the multiple collision of the fast neutrons with light hydrogen atoms in the water moderator thus slowing it down. Although heavy water has a much lower neutron absorption capability, light water is preferred in PWRs because of its effective neutron moderation property and its availability.

#### **1.2.1.1 European Power Reactors (EPR)**

The EPR is a Generation III+ evolutionary four-loop Pressurised Water Reactor (PWR). It was developed by Framatome and Siemens in partnership with the Nuclear Power International (NPI). It received technical support from the French utility Electricité de France (EDF) as well as from the German utilities who financed most of the development work (AREVA, 2012). The main components of the EPR design, loop configuration and primary system design, is not any different from operating PWR designs around the world.

#### **1.2.1.2 EPR Design Overview**

The EPR components entails ; the four-loop pressurized water Reactor Cooling System (RCS), the reactor vessel containing the fuel assemblies, a pressurizer to maintain system pressure, Reactor Coolant Pump (RCP), steam generator and control and protection systems. These components are shown in Figure 1.1 below.

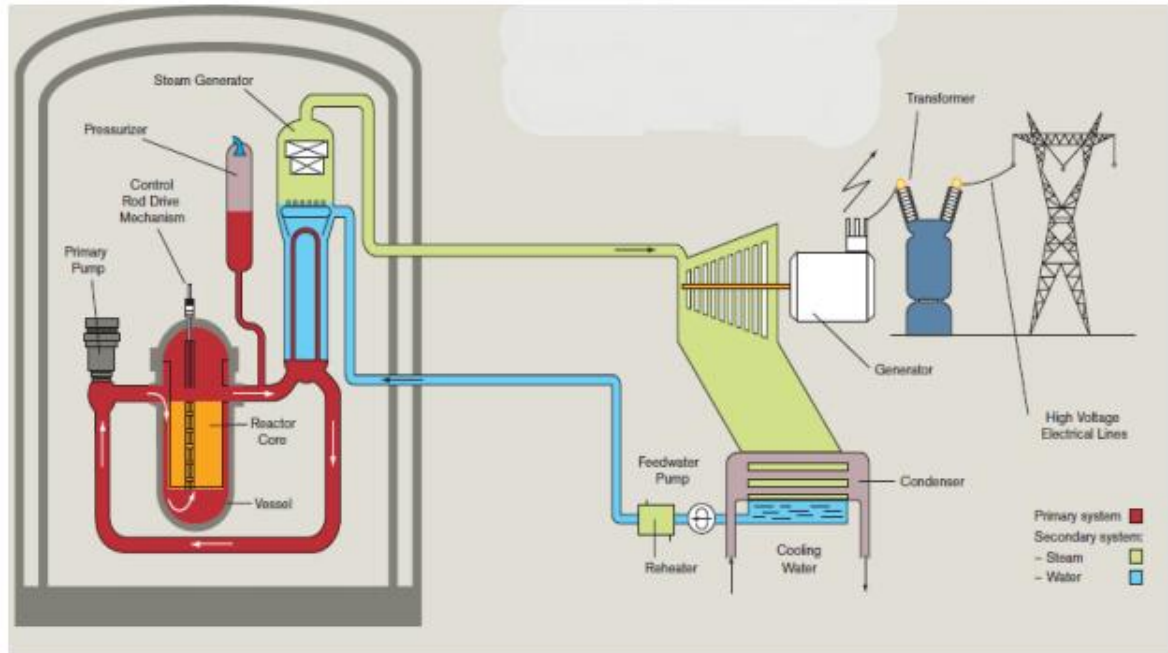


**Figure 1. 1 EPR Plant layout**

The EPR uses light water as both moderator and coolant to remove heat produced as a result of the fission process in the reactor core and slow down fast fission neutrons born from the fission reaction in the core respectively. Slowing down the fast neutrons is important so that the neutrons are brought to thermal energies to be able to interact with the fissile atoms in the fuel to sustain the fission. The heat generated from fission in the core is carried by the primary coolant into the steam generator to be transferred to the secondary loop by the steam exchangers. The steam generated in the secondary loop is then pumped to drive the turbines to generate electrical energy (AREVA, 2012).

The EPR has new features like the redundant (passive) emergency core cooling system, shield and containment building and a core melt catcher in case of accidents. The volume required to contain the reactor core, heavy reflector, flow directing and supporting internals and the control rods is provided by the Reactor Pressure Vessel (RPV) with a diameter of

438.5 cm (AREVA, 2012). The reactor pressure vessel has thick walls made of low carbon alloy steel and internals made of NiCrFe alloy cladding to withstand the high operating pressures and increase resistance to corrosion. Within the RPV are four outlets and four inlet nozzles to provide connections to the four loops circulating the reactor coolant as shown in Figure 1.2 below.

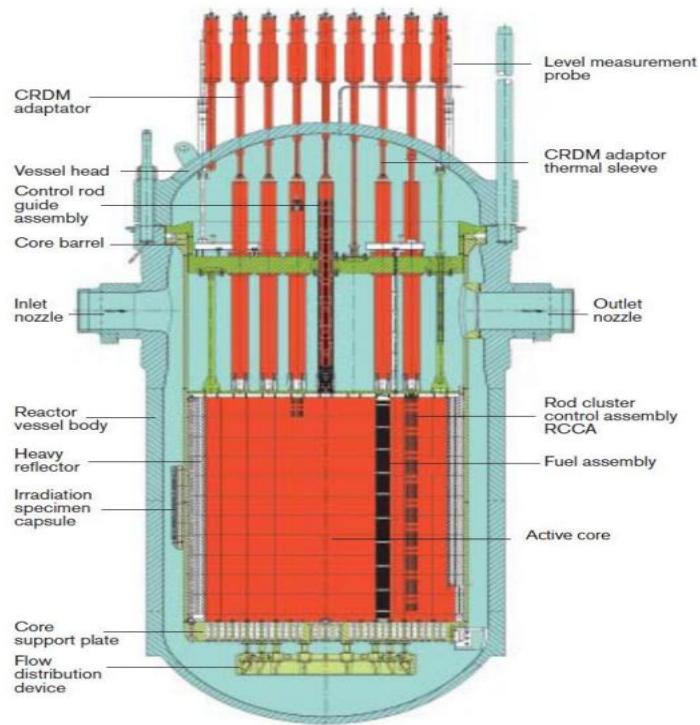


**Figure 1. 2 EPR Reactor Pressure Vessel**

The reactor has a core with an active height of 420 cm and a rated thermal power of 4,500 MWt. The core is designed to have a high thermal efficiency, low fuel cycle cost, and flexibility for extended fuel cycle lengths. The core cycle length is determined by the energy output required with the life time ranging from 12 to 24 months. The reactor core consists of 241 fuel assembly arrays. The fuel assemblies are arranged into a pattern to form a cylindrical shape. To avoid neutron escape in the core, a heavy reflector which is a

large steel structure of 10.2 to 20.3 cm width, surrounds the edge of the active core. This heavy reflector also flattens the core power distribution and reduces the effects of the fast neutrons on the reactor pressure vessel (AREVA, 2012).

The fuel assembly has a 17 x 17 lattice design with 265 fuel rods, 23 guide tubes. The fuel rod consists of cylindrical shaped uranium oxide (UO<sub>2</sub>) pellets encapsulated in a zirconium alloy tube with plugs welded at each end. The zirconium alloy cladding offers resistance to corrosion associated with the high operating temperatures and high burn-up. The gap between the fuel meat and cladding offers an acceptable margin for failure due to pressure build up. The pellets are enriched up to a value of 4.95 %wt. U-235 with tolerance of about 0.05%. The Rod Cluster Control Assembly (RCCA) each consists of 24 individual absorber rods fastened to the assembly arrangement. Silver (Ag) is the largest constituent of the absorber rod with 80 %wt. and Indium (In) and Cadmium (Cd) making up 15% and 5% respectively. The absorber material is sealed in a 316L type stainless steel cladding tube to protect it against the coolant (Framatome ANP, Inc., 2005).

The RCCA are used for shut down and control purposes.

Chemical absorbers are also used to control reactivity in the reactor. Typically, Boron which is diluted in the moderator as boric acid is used as a chemical absorber in the EPR. The boron content is limited by the moderator coefficient.

### **1.2.1.3 Hualong One Pressurized Water Reactor (HPR1000)**

The Hualong One Pressurized Water Reactor (HPR1000) is an active and passive advanced PWR which meets the requirements of Gen-III nuclear power plants in terms of technical

maturity, safety and economic competitiveness (CNNC, 2015). The HPR-1000 was designed by the China Zhongyuan Engineering Corporation under the supervision of the China National Nuclear Corporation (CNNC).

The HPR demonstration project was commenced on the 7<sup>th</sup> of May 2015 when the China National Nuclear Safety Administration (NNSA) issued construction permission on the same day after reviewing the preliminary safety analysis report (PSAR). “The basic safety to be achieved in the design of HPR-1000 is control of the reactivity, removal of heat from the core and spent fuel, and confinement of radioactive materials and control of operational discharges as well as limitation of accidental releases” (CNNC, 2015).

#### **1.2.1.4 Design Overview of the HPR-1000**

The reactor pressure vessel (RPV) is one of the most important parts in the reactor coolant system pressure boundary and is equally important in shielding against radioactivity. The RPV also houses the reactor core, reactor internals, core support structures and some measuring and control components. The reactor pressure vessel is composed of three parts : closure head, vessel body, fasteners and shell parts.

The heat from the reactor core is transported through the reactor coolant system to the steam generators where the heat is transferred to the secondary system to produce steam that will be pumped to turn turbines. The reactor coolant system consists of three similar heat transfer loops connected in parallel to the reactor pressure vessel. Each loop contains a reactor coolant pump and a steam generator. The reactor coolant pumps serves to circulate pressurized water through the reactor vessel and the coolant loops during operation. The

reactor coolant water serves as moderator and also as solvent for the boric acid as it passes through the core (CNNC, 2015).

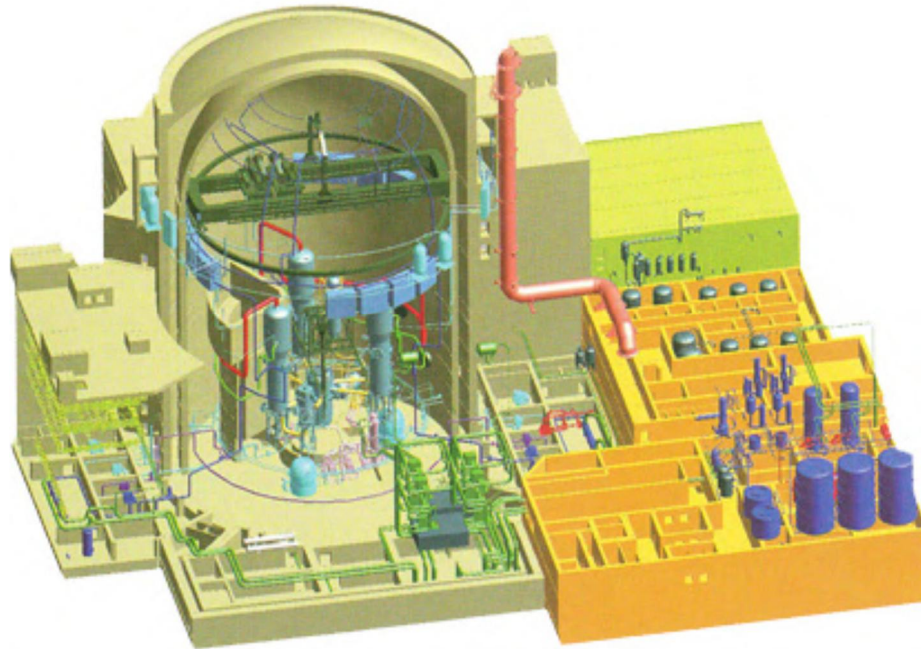


**Figure 1. 3 HPR plant layout**

The reactor core consists of 177 fuel assemblies, which has an active core height of 365.8 cm, and an equivalent diameter of 322.8 cm. Fuel assemblies of three enrichment are used in the initial core, which are 1.8%, 2.4% and 3.1% respectively. Two regions consisting of the two lower enrichment are interspersed so as to form a checker board pattern in the central portion of the core. The third and highest enrichment is arranged around the edge of the core.

The core is designed to be loaded with CF3 fuel assembly. CF fuel (china fuel) series include CF1, CF2 and CF3, with N18 and N36 Zircaloy cladding (Guanxing, 2012). The

CF3 fuel assembly is composed of 264 fuel rods arranged within a 17x17 supporting structure.

Fuel rods are slightly enriched sintered uranium oxide pellets contained in a closed tube, hermetically sealed at its ends by wedged end plugs. The gap between the pellet and the cladding, the initial pressurization and density of the pellets are calculated so as to minimize interaction between the pellet and the cladding (PCI). The guide thimbles are structural members which also provide channels for the control rods, neutron absorber rods, burnable poisons rod (for the first core), and neutron source or thimble plug assemblies.

Also, among the core components are the rod control cluster assembly made up of neutron absorber rods fastened at the top end to a common spider assembly. The RCCA are used for shutdown and control purposes in cases of fast changes in reactivity.

In nuclear power reactors, changes of temperature affect the reactivity in many ways. Changes in reactivity due to moderator temperature changes, fuel temperature changes and changes in void content make up the total reactivity coefficient. In PWRs working at steady state, change in reactivity due to moderator temperature changes is the most important. Reactivity changes due to change in void content is less significant in a PWR working at steady state. However, this becomes very necessary when simulating a loss of coolant (LOCA) situation. Overall, the contribution of the fuel temperature of reactivity to the total is very small but the fluctuation in temperature gives information on fuel oscillation (Aguilar & Por, 1987).

### **1.3. Objectives**

#### **1.3.1 Main**

- Determine the radiotoxicity of spent nuclear fuel of the two reactors at end of fuel cycle (EOC) up to a million years.

#### **1.3.2 Specifics**

- Determine the Fuel burn up to obtain the final composition of the spent nuclear fuel. The computational code MCNPX version 2.7 will be used to determine the isotope constituent of the spent nuclear fuel assembly.
- Compare the radiotoxicity of the SNF with and without the actinide that are major contributors to the radiotoxicity and make recommendations.
- To compare the radiotoxicity of the SNF from the two reactor and make recommendation on choosing a particular nuclear technology.

### **1.4. Scope of Study**

This study will be concentrated on the radiotoxicity analysis of spent fuel assembly of the two considered pressurized water reactors. Only radiotoxicity by ingestion is considered.

The reactors to be considered in the study are the Chinese HPR, and the French EPR nuclear reactors.

The MCNPX version 2.7.0 code will be employed as a computational tool to help obtain the results.

### **1.5. Organisation of the Research**

The entire study was organized in six chapters. The first chapter focused on the background of the study, research problem, research justification, research objectives, and scope of the study and organization of the research.

The second chapter discussed works in related fields that were relevant to the study. Chapter three discusses the theoretical background of the study. It then proceeded to chapter four which focused on the methodology and fundamental equations used in the design and simulation process.

In chapter five, data from the simulation were analyzed and discussed. The research concluded in chapter six with the conclusions and suggestions for future study.

This chapter has given the overview on radiotoxicity of SNF and its origin. The historical background of the study, the research problem, justification of research, the objectives, and scope of the study was also discussed.

In the next chapter, review of the past related works, relevant to this study is done.

## CHAPTER TWO

### 2.0 Literature Review

This chapter serves to analyse and review the previous works that are related to this study.

### 2.1 General

Closely related to the application of nuclear energy for power supply are the beneficial and detrimental effects just like any natural resource means used for power generation.

The harmful effect arises from spent nuclear fuel (SNF).

It is vital to get information on the development of material constituent and radionuclide inventory with time during which the reactor is being operated. Such information will help to estimate the entire radioactive hazard (i.e radiotoxicity) that could originate from these fuels when it is spent.

### 2.2 Previous Related Works

#### 2.2.1 MCNPX

Before the development of MCNPX for depletion calculations, monte carlo based methods have been used in the past for nuclear fuel management analysis. An example is the MONTEBURNS code which works together with ORIGEN for depletion calculations. The following reviews describe the development of the MCNPX code, and its validation for use in fuel management.

López and Töre, 2007, performed a study to compare the code MONTEBURNS, (a new code at the time, developed in Los Alamos Laboratory), with ORIGEN-S for the WWER fuel rod isotopics calculation in an infinite array at different burnups of 10, 30 and

40MWd/KgU (López & Töre, 2007). After the simulation was conducted for a cycle duration of 365days, the results showed a relative error lower than ten percent but with the exception of some radionuclides which includes Am-243, Gd-155, Sm-149, Sm-151 and Sm-152. For the Samarium isotopes and Gd-155 there are some undefined resonance regions in the ENDF cross-section libraries, which could be the reason of the big differences according to the deduction from the study. Based on the relative error in the results, the study concluded that MONTEBURNS is less accurate as compared to ORIGEN-S for depletion calculations. However, MONTEBURNS may become a very important tool for isotopic studies in the future because its accuracy depends on the quality of the cross-sections used. MONTEBURNS is a precursor to MCNPX. MCNPX has an updated cross section library.

Kalcheva and Koonen, 2007, performed a study to check the accuracy of the Monte Carlo burnup code MCNPX 2.6C against the already established MCNP and ORIGEN method at the time ( Kalcheva & Koonen, 2007). The Material Testing Research Reactor in Mol, Belgium was used as case study. Burnup and depletion calculation results from MCNPX 2.6C/CINDER'90 were compared to results from MCNP and ORIGEN. The MCNPX 2.6C and CINDER'90 process is automatic and the steady-state flux calculations by MCNPX are internally linked with the depletion calculations by CINDER'90. So, the reaction rates are updated for each burn time step. In the MCNP and ORIGEN-S method, the reaction rates are calculated by MCNP once, at the beginning of core life, and introduced to ORIGEN-S. ORIGEN does the depletion computations for the wanted time steps. The power peaking factors and  $K_{eff}$  would then be able to be assessed for each burn step separately and at the same time. Due to this strategy, MCNP and ORIGEN-S require less

computational cost. However, MCNPX 2.6C and CINDER'90 can burn a boundless measure of materials, whereas, MCNP and ORIGEN is constrained to 4,000 materials (Fensin M. L., 2008). From examination of calculated reactivities, criticality, and nuclear densities, the paper verified that the precision of MCNPX and CINDER'90 is lower, compared to MCNP and ORIGEN-S. Furthermore, the MCNPX 2.6 code is continually developing and its accuracy depends on the cross-section library used.

Boafo, et al., 2014, performed a study to investigate the fuel depletion for a potential Low Enriched Uranium core of Ghana's Miniature Neutron Source Reactor (GHARR-1) utilizing the Monte Carlo N-particle extended (MCNPX) neutron transport code (Boafo, Alhassan, & Akaho, 2014). The method involved introducing a Burn card to the already existing input file for both the HEU and LEU cores. The ENDFB/V-II.0 cross section library was used for the isotopes. The CINDER library file was also used in the study by MCNPX for the depletion calculations. It contains both decay and fission yield data, needed to achieve the depletion simulations. Depletion study was done for the reactor center from the beginning of life (BOL) to the end of life (EOL) which amounts to 10 years of reactor operation history. An estimate of the amounts of the major actinides at BOL and EOL of the core, was determined. The rate at which the MNSR removes decay heat after reactor shutdown was also studied because of its importance to reactor security and safety. Fission products delivered after burnup was likewise ascertained. The outcomes of the study demonstrated that a 0.568 percent of U-235 was devoured at EOL i.e. after operating the reactor for two hundred days at full power. Also, a non negligible measure of Pu-239 was delivered for the LEU core while a negligible amount was produced for the HEU core. The result is shown in Figure 2.1 below.

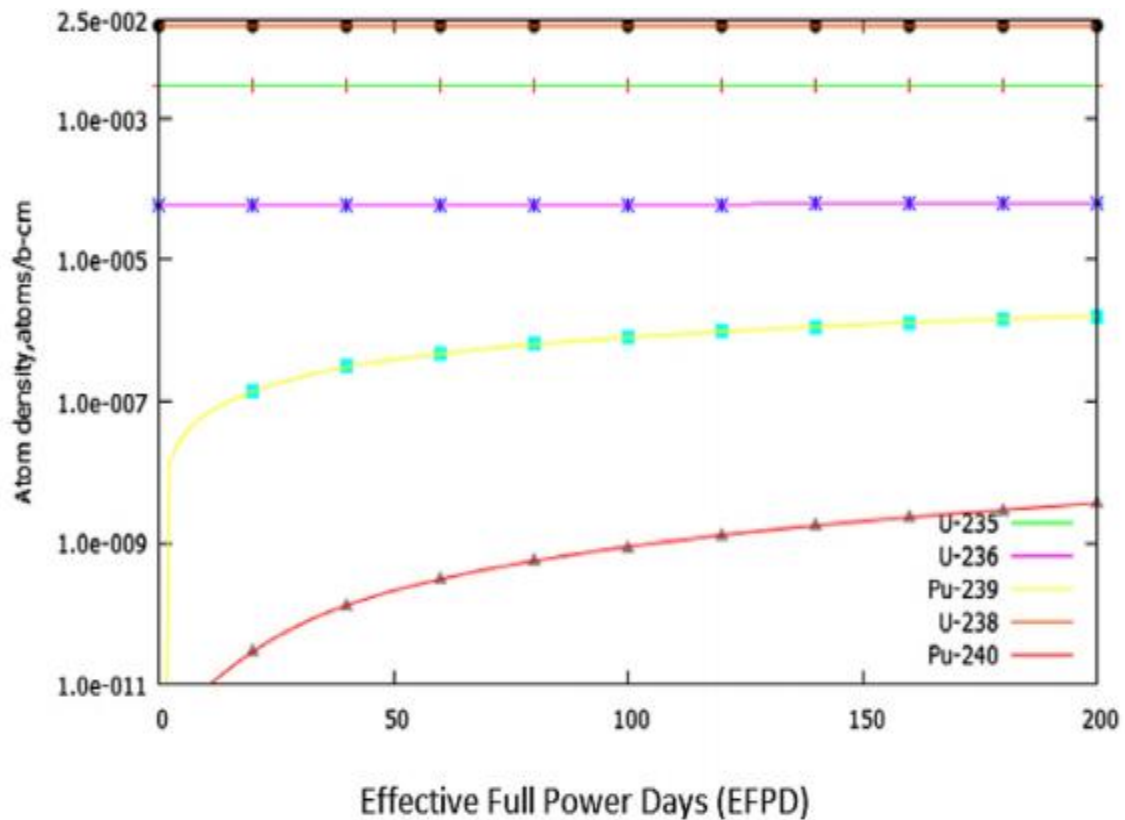


**Figure 2.1 Result showing Atom density of various actinides as a function of Effective full power days. (Boafo, Alhassan, & Akaho, 2014)**

From the results from the study, it was also observed that the decay heat shows an exponential decrease after reactor shutdown. This implies that decay heat will be removed in the system by natural circulation which is good omen for the safety of the reactor (Boafo, Alhassan, & Akaho, 2014). After comparing of the outcome of the study to other similar works using other codes, consistency was observed. The results from the study has demonstrated the capability of MCNPX for depletion calculation of a Miniature Neutron Source Reactor.

Cao, et al., 2010, performed a study to compare the Isotope Correlation Experiment ICE data of the NPP obrigheim to the MCNPX simulated analytical data (Cao, Gohar, & Broeder, 2010). The ICE-Experiment was an experiment that was performed in Germany

for the Obrigheim NPP way back in the early seventies. The reactor is a Pressurized Water Reactor (PWR) having an enrichment of 3.1% enriched  $\text{UO}_2$  fuels. Five fuel assemblies were irradiated in the first two fuel cycles. They were unloaded in the next cycle, and later reloaded and irradiated for one more fuel cycle in the experiment. The Monte Carlo simulation results were compared with the ICE Experimental results for burnup up to 30 GWD/t. The methodology involved modelling a pin cell to simulate the fuel lattice of the nuclear reactor. Temperature dependent libraries based on JEFF3.1 nuclear data files were used for the calculations in order to do comparison with the ICE-data at 1273<sup>0</sup>C, 973<sup>0</sup>C and 973<sup>0</sup>C for the fuel, the clad, and the moderator regions, respectively. ENDF/B-VII cross section library was used for the simulations to investigate the possible differences due to using different cross section data files. The results obtained were very close to the JEFF3.1 results, except for 10% differences in the prediction of the minor actinide isotopes buildup. The result revealed that MCNPX can predict correctly the depletion of uranium fuels. Also the burnup values showed good correlation with the ICE experiment results for depleting U-238 where the maximum error was 0.09%. Also, U-236 atom density buildup simulation result was underestimated by MCNPX because the results do not agree well with the ICE experimental result for each burn step. The plutonium isotopes showed good correlation with the ICE experiment data. Due to limitations in the ICE technique, the ICE-Experimental data points were very inaccurate for results obtained for the Am-241 and Am-243. MCNPX results were also more than 100% inaccurate at most of points in time for both of these Americium isotopes. The differences from the results between the analytical calculations and the experimental measurements for the curium isotopes was around 20%, which was far more better correlation than for the americium isotopes. For the fission

products, there was much agreement in comparison of both approaches. It was concluded from the study that MCNPX code has the capability to accurately predict the U fuel depletion and the Pu production and the buildup of most of the fission products in a thermal reactor. The simulation results agree with the ICE measurements within the experimental uncertainties. The only exceptions are for U-236 and Pu-238, the largest deviations from the experimental data are 4%, and 20%, respectively. This was due to large error bar from the ICE experiment for Pu-238. Also the MCNPX predicted accurately the atom densities of the fission products except for a deviation of 6% for the Kr-84/Kr-83 isotopic ratio, 15% for Kr-84/Kr-86, 20% Nd-144/Nd-148 and 6% for Nd-143/Nd-148 from the ICE measurements. In addition, the comparison of the results using JEFF3.1 and ENDF/B-VII showed negligible differences. The study has validated MCNPX code for depletion calculations of UOX spent fuel.

### **2.2.2 Radiotoxicity**

Information on the isotope constituent of nuclear fuel at end of cycle is very relevant in different applications. For example ; in the modelling of decay heat after reactor is shut down ; to investigate fuel pin failure to identify the position of any ruptured fuel pin ; for proper spent fuel management strategy.

In this study, information on the isotope constituent of the spent nuclear fuel will be directed at estimating its radiotoxicity at end of cycle up to a million years. Previous works have also been done in the past in this area either using MCNPX or other codes. The following reviews describe them.

Sogbadji, et al., 2016, performed fuel management study aimed at reducing the actinides concentration of nuclear fuel waste. The MURE code was used to design the uranium oxide fuel (UOX) assembly of a typical French pressurized water reactor to reach a burnup of 46 GWd/T and 68GWd/T (Sogbadji, David, Akaho, & Nyarko, 2016). MURE stands for MCNP Utility for Reactor Evolution. MURE is based on C++ programming. This allows great flexibility in its use. The code performed a reactor time evolution utilizing the particle transport code MCNP. The MURE code depends on the linking of the Monte Carlo code and the estimation of the evolution of the nuclear fuel amid irradiation and cooling times.

Reprocessing of spent UOX was done to create mixed oxide MOX fuel assembly. This was achieved by extracting plutonium and including depleted uranium. Simulation was then performed to reach burnups of 46GWd/T and 68GWd/T. Impacts of different cooling times of the spent fuel assembly was also considered. It was observed that after thirty years cooling time in the storage, the spent UOX fuel required a higher concentration of Plutonium to be reprocessed into Mixed Oxide fuel due to the decay of Pu-241. A strategy was proposed for reprocessing the americium isotopes, which now dominated the radiotoxicity of the waste. The mixed oxide and americium isotope, MOXAm fuel was then created to check the impact of americium in mixed oxide fuel on the neutronic characteristics, burnup and radiotoxicity. In the study, the graphic user interface of MURE was utilized to calculate the radiotoxicity of the isotope development of the nuclear fuel. The results from the study showed that the high level of Pu in the MOXAm (mixture of PuO<sub>2</sub>, UO<sub>2</sub> and AmO<sub>2</sub>) fuel, which is as a result of Am buildup in the fuel, the radiotoxicity of the MOXAm fuel with longer cooling time and longer burnup from the UOX cycle from which they were reprocessed from, relatively maintained their

radiotoxicity as compared to the open cycle from which they were fabricated from. The result from the study has demonstrated the ability of the MURE code to calculate depletion, decay and radiotoxicity calculations. Also, the mono recycling of americium does not have considerable reduction in radiotoxicity as compared to the open cycle.

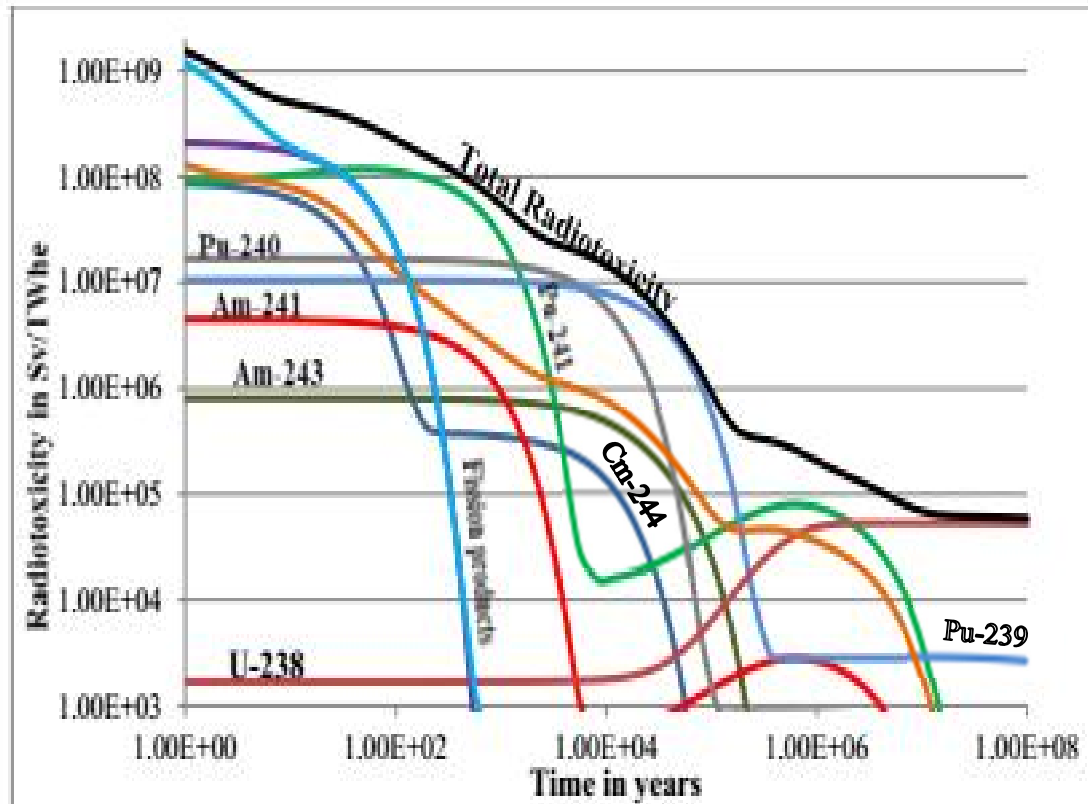


**Figure 2. 2 Sogbadji, et al 2016., Result of Radiotoxicity Calculation for UOX fuel of French EPR at burnup of 46GWd/t.**

Salome et al., 2016, investigated and analyzed the released SNF of 3 types of nuclear technology which includes a standard pressurized water reactor PWR, a high temperature gas reactor VHTR and lead cooled accelerator driven system ADS to investigate their radiotoxicity and decay heat (Salome, et al., 2016). The fuel burnup information for the systems in different works were utilized for the examination of the spent fuel. The

radiotoxicity and the decay heat were evaluated using the ORIGEN2.1 code (Salome, et al., 2016) until  $10^7$  years. ORIGEN is a code used in determining the buildup, decay, and processing of radionuclides. The result from the study showed that SNF obtained from reprocessing techniques and used as fuel in advanced reactors showed a decrease in radiotoxicity as compared to the conventional SNF from a typical PWR operating an open cycle system. The ADS and VHTR has high radiotoxicity and decay heat values due to build up of plutonium and curium in them. The highest contribution of fission products to radiotoxicity was observed from 0 to 25 years, the most radiotoxic being Ba-137, Tc-99 and I-129 while for actinides, plutonium and curium contributes highest. The results from this study has demonstrated the efficacy of ORIGEN code in calculating the radioactivity, radiotoxicity as well as decay heat of SNF. The decay heat parameters can be used to design canisters used for storage of SNF.

Arafat, et al., 2011, performed Radiotoxicity Characterization of high level waste produced from Reprocessing of Uranium and Thorium Based Fuel through SCALE depletion calculations (Arafat, et al., 2011). SCALE is a modeling and simulation code for nuclear safety study and design to perform reactor physics, radiation shielding, criticality safety and spent fuel classification for nuclear facilities and transportation and storage package designs. (<https://www.ornl.gov/scale>, n.d.). Decay calculations were performed with ORIGEN to determine the spent fuel overall radiotoxicity as well as the critical contributors (progeny and parent) at the various time ranges for both Uranium oxide UOX and thorium oxide ThOX nuclear fuel. In the study, with the SCALE code used, the outputs have to be input into ORIGEN for depletion calculations. An exception is when higher versions of SCALE which is ORIGEN integrated (e.g. SCALE 6.2.1) is used. The results showed that

there is similarity in radiotoxicity level for the Uranium-MOX and Thorium-MOX up to 20,000 years which is in contrast to the radiotoxicity level of the ThOX which is lower in the intermediate to long term range as compared to UOX. Reason being that the plutonium content in Thorium-MOX is directly responsible for the radiotoxic content. The reactor grade and weapons grade plutonium from the MOX fuels were also compared. It was shown that the radiotoxicity of the Weapons grade Pu was lesser than that of the reactor grade plutonium which implies that there was more neutron capture processes in the reactor grade than in the weapons grade plutonium which has a lesser Pu isotopes content. The study concluded that thorium-based fuel is more promising since it generates more acceptable HLW and also producing U-233 which is fissile and can be used as fuel. The significance of the study on radiotoxicity for first thermal recycle fuel having varying content of fissile and fertile materials will guide the development of a multiple tier system and advanced reactors towards generating acceptable HLW. The study has also demonstrated the use of SCALE for depletion and radiotoxicity calculations.

Francois, et al., 2009, studied Impact of Actinides Recycling on Radiotoxicity for Boiling Water Reactors Fuel. The production rate, the destruction rate, and also the radiotoxicity of Pu and minor actinides (MA) which were obtained from the multi-recycling of boiling water reactors (BWR) fuel were examined. The method involved designing a BWR Mixed Oxide fuel assembly, containing uranium, plutonium and minor actinides and its characteristics studied using the HELIOS code (Francois, Guzmán, & Campo, 2009). Helios is a deterministic computational code using the transport theory. The study showed comparison of the actinides mass and the radiotoxicity of the spent fuel with those of the open cycle. Four cycles, each 18 months in length was used, thus giving a burnup of 48

MWd/kg (Francois, Guzmán, & Campo, 2009). The result showed that the radiotoxicity of the recycled fuel is higher than that for the direct cycle until a few hundred years. It was also revealed that the radiotoxicity of the spent fuel from the first recycling was lesser around a hundred years as compared to the second recycling. From hundred years and above the radiotoxicity of the second recycling was now lesser. This was because of the higher concentration of Cm-244 in the spent fuel of the first recycling. Cm-244 is highly radioactive but have short half life therefore, during the first tens of years after the fuel discharge, the radiotoxicity of the recycled fuel was higher than that of the direct cycle. Minor actinides (MA) recycling alone without plutonium was also considered and its impact on radiotoxicity examined. It was revealed that in the period between fuel discharge until some thousands of years, the radiotoxicity of this fuel was smaller than that of the MOX fuel containing Pu, minor actinides (MA) from the first recycling and uranium tails. Nevertheless, afterwards, the radiotoxicity of the fuel reached the toxicity level of the spent fuel from direct cycle, and becomes higher than the radiotoxicity of the fuel with Pu and MA. From the results of the study, it was concluded that the highest reduction in radiotoxicity for the open cycle up to a thousand years after discharge is from the fuel containing minor actinides and enriched uranium, with the plutonium extracted. The lowest radiotoxicity after few thousands of years is from the fuel with plutonium and Minor Actinides. The study concludes that reprocessing of major and minor actinides in SNF reduces the radiotoxicity. The increase in the number of recycling leads to further reduction in the radiotoxicity. Higher reductions in radiotoxicity can be obtained in reactors with fast neutron spectrum and with accelerator driven systems. The study has shown the efficacy

of recycling in reducing radiotoxicity and also demonstrated the ability of the code HELIOS for depletion and radiotoxicity determination for SNF.

Joe, et al., 2012, performed a study to determine the Pu isotopes composition for a high burnup PWR fuel samples using both alpha spectrometry and mass spectrometry. This was done after anion exchange separation. The results derived from measuring were compared with results simulated by the ORIGEN2 code. The method involved analysing seven high burnup pressurized water reactor (PWR) spent fuel samples with burnup ranging from 33.21 to 59.03 GWd/MtU (Joe, et al., 2012). Based on the properties of the isotope, the contents of the plutonium isotopes were determined using alpha spectrometry and mass spectrometry where appropriate, and these contents were evaluated by a comparison with the results calculated by the ORIGEN-2 code. The burnups of the fuel samples used to calculate the plutonium isotope contents were determined by a chemical method using Nd-148 as a burnup monitor. From the results, it was revealed that the measured values were slightly higher than the calculated values, within about 10% except for Pu-238 and Pu-242. For Pu-238, the difference between the measured and calculated values was over 20% on average. The exact reason was not identified. The study concludes that after comparing the measured value and the calculated value by the ORIGEN-2 code, the measured counts were a little bit higher than the calculations like 10% higher. What gave this higher value was not determined. Assumption as to what could have caused it were measurement uncertainties or the input libraries in the ORIGEN-2 code such as neutron flux and the burnup value for the spent fuel. After comparing the standard benchmark for isotopic composition of Pu in high burnup PWR spent fuel samples, the result showed that the correlations derived in this study also worked well for other high burnup PWR spent fuel

samples, to within an acceptable error range. Therefore this study qualifies as benchmark for codes evaluation.

Bergelson, et al., 2005, conducted a research to study the radiotoxicity of one tonne of SNF from a VVER type reactor during storage time up to 300,000 years. From The methodology used, calculations were done individually for the fission products and actinides and Isotopic constituent of actinides and fission products in spent fuel were determined at fuel burnup of 40 MWd/kg with 3 year cooling time (Bergelson, Gerasimov, & Tikhomirov, 2005). Assumption made was that uranium had been removed from SNF and only Np, Pu, Am and Cm were transferred into the repository. The 300,000 year storage time was used. In determining the radiotoxicity by ingestion and inhalation, the maximum permissible activity of nuclides in drinking water and air was used. In this study radiotoxicity was determined as the volume of air or mass of water required for the dilution of a given amount of radionuclides to permitted levels of concentration. From the result it was revealed that inhalation radiotoxicities of actinides is more than that from fission products while ingestion radiotoxicities of fission products is higher than for actinides at storage below 20years. With further storage time, radiotoxicity contribution from fission products decreased rapidly while that for actinides decreases slowly with time. The study concluded that if an open cycle were to be employed the SNF can be stored without separating the constituent since it has been established that plutonium is the major contributor to the radiotoxicity. The study further concluded that when a closed cycle is employed, the SNF can be separated and plutonium can be reused as fuel, while the major fission product contributors to radiotoxicity i.e Cs-137 and Sr-90 can be controllably stored for several hundreds of years to decay. Also, the rest of the fission products having very long half life

can be transferred to the final repository. The study also suggests the transmutation of Am-241 whose contribution to radiotoxicity is also very high and has longer half-life than Cm-244 which decays in a hundred years.

Necas, et al., 2005, carried out a study to compare the radiotoxicity of three models of fuel assemblies for various nuclear fuel cycles. The model includes a standard uranium fuel assembly, a mixed oxides (MOX) fuel assembly, and an inert matrix combined fuel assembly. The method involved modelling the burnup of the VVER-400 fuel assemblies using a standard UOX, the MOX and the inert matrix combined (IMC) fuel assemblies to reach burnup of 40,000MWd/MTU using the code HELIOS, after which the spent fuel inventory (to determine the actinides and fission products in the SNF) was calculated with the code ORIGEN (Necas, Sebian, & Kocisk, 2005). The assemblies were assumed kept in spent fuel pool for five years to cool. The radiotoxicity was calculated as ;

$$R(\text{Sv}) = \text{DCF}(\text{Sv/Bq}) \times A(\text{Bq}) \quad (2.1)$$

The result indicated that about 35% long term risk reduction was obtained for the IMC fuel assembly as compared to the standard UOX fuel assembly, while the risk was 2.5 times higher for the spent MOX fuel assembly FA. This high risk amount in MOX fuel assembly attributed to the high initial Pu enrichment and Transuranics production from U-238. The mass of the Pu-239 at the end of U-FA burn-up was 6.26 g per fuel pin but at the IMC-FA it was only 0.97 g per fuel pin. The Pu-239 mass was reduced down to 15.5% by transmutation, but as for the MOX-FA the mass of Pu-239 increased up to 3.32 kg per assembly. In comparison with the uranium fuel assembly which was 0.789 kg per assembly, it was 4.2 times higher. It was also revealed that the risk due to Np-237 and Cm-

<sup>244</sup>Pu in the spent fuel assembly of standard uranium was higher for a closed fuel cycle, while for the inert matrix spent fuel assembly, the risk was reduced. The study concluded that the inert matrix combined fuel assembly is a much more effective tool for plutonium mass reduction than the MOX fuel assembly. Also, closed fuel cycles exhibit reduction of residual hazard index for plutonium but an increase in this indicator for higher actinides. It was further concluded that the simulation of the transmutation process for the three various assemblies in the core of the LWR reactors studied showed significant transmutation potential. The study identified the need for a correct approach to determining radiotoxicity in order to select appropriate waste management methods.

There are several computational codes available for use in fuel management analysis which could be based on either deterministic methods or Monte Carlo methods.

Deterministic methods basically solve the neutron transport equation for the average particle behaviour. The relation of the output to the input is determined decisively. Further elaboration on deterministic methods can be found in chapter three of this study.

Stochastic methods or Monte Carlo do not solve the transport equation like the deterministic method based codes mentioned above, but rather simulates particle transport for each particle, tracking the path of each individual particle throughout its life time and recording the average behaviour of these particles. A large number of particle trials or histories are required to accurately describe the phenomenon.

Monte Carlo (MC) techniques, contrasted with deterministic techniques, are appropriate for complex three-dimensional, time dependent problems. Monte Carlo method permit correct geometry details. Also, MCNP uses point-wise cross sections which follow the true

cross sections as a function of energy. Cross sections for most nuclides are included in libraries used by MCNPX. Deterministic methods require group-wise cross sections, which are based on energy groups. Group-wise cross sections are created from collapsed/averaged continuous cross section libraries. While group-wise cross sections allow faster calculations, calculations using group-wise cross sections are not as accurate as calculations using point-wise cross-sections. MCNPX allows creation of geometries by specifying surfaces that define the boundaries of volumes called cells. Cell characteristics such as temperature, material, density, and particle importance are specified, and materials are defined by their constituent nuclides and respective mass or atom fraction. An appropriate cross section library is specified for each nuclide. In addition, MCNPX uses the Visual Editor program to verify and easily locate geometry errors visually.

The present work utilizes MCNPX version 2.7 which has an updated cross section library for isotopes and nuclei reactions thus will generate more accurate results. The present work focuses on depletion calculation of spent nuclear fuel assembly to study its radiotoxicity.

This chapter has reviewed related works on radiotoxicity and simulation of burnup and depletion of nuclear fuel as well as decay of the spent nuclear fuel. The merit of MCNPX as compared to other codes for depletion and burnup calculation has been briefly highlighted. There is further discussion on MCNPX in the next chapter.

The next chapter describes the relevant theoretical aspects that applies to utilizing MCNPX for depletion calculation of spent nuclear fuel assembly in order to estimate its radiotoxicity.

## CHAPTER THREE

### 3.0 THEORETICAL ANALYSIS

#### 3.1 Introduction

This chapter and the subsequent sections introduce the Monte Carlo method MCNPX for burnup calculation. It also covers the basic nuclear reactor theory and the required reactor physics and also the fundamental equations governing the depletion of isotopes which serves as the background to the applied Monte Carlo technique's (i.e. MCNPX's CINDER integrated) depletion capability.

#### 3.2 Nuclear Reactor Theory

In a steady state radiation field, the net rate at which particles are lost in an element must be exactly balanced by the rate of secondary or source particles which are introduced into the volume. The linear particle transport equation or linearized Boltzmann transport equation is used to determine the particle distribution in space,  $r$  direction,  $\Omega$  and energy,  $E$  in plane, spherical or cylindrical geometry. The equation is the basic physical model to describe the transport of uncharged particles such as photons ( $\gamma$  – rays, light, etc.) and neutrons.

Calculations of conditions necessary for criticality are normally carried out using the group diffusion method. The one-group diffusion method gives only the roughest estimates of the properties of a critical reactor and is most appropriate for a fast reactor (Larmash, 2001). For convenience, all materials other than the fuel are considered as moderator for one-group calculations. The thermal reactor system contains fuel, coolant, various structural materials, and a moderator to slow down the fission neutrons to thermal energies. The

several regions with different material properties are represented by a set of equations. In this case, it is important to solve the equations in each region and satisfy the boundary conditions at every interface and at the reactor surfaces. To obtain accurate results, the multigroup diffusion method is employed. The procedure can only be carried out in a practical way with a high-speed computer, and there are many computer programs written for solving the multigroup equations (Larmash, 2001).

### 3.3 Neutron Transport Theory

The physics of the requirements of a nuclear reactor core is determined by the description of production, transport and absorption of neutrons in the core. Neutrons move about in a reactor in complicated paths due to repeated collisions with nuclei, making it difficult to predict the distribution of neutrons in space, energy and time. The equation governing this neutron transport phenomenon is called the neutron transport equation, which expresses the distribution of neutrons in space, energy and time in a straight forward manner. The transport equation is important to calculating the conditions necessary for criticality in a reactor, such as the spatial distribution of neutron flux at various energies and other quantities which form the basis of nuclear reactor design. In principle, the prediction of the distribution of neutrons can be done by solving the neutron transport equation. Various approximations are used and numerical solutions are obtained by computational procedures. The general form of the transport equation can be written as (Glasstone, 1994);

$$\left[ \begin{array}{c} \text{change in} \\ \text{neutron density} \\ \text{with time} \end{array} \right] = \left[ \begin{array}{c} \text{change due to} \\ \text{physical changes} \end{array} \right] + \left[ \begin{array}{c} \text{change due} \\ \text{to collision} \end{array} \right] + \left[ \text{sources} \right] \quad (3.1)$$

this is expressed mathematically as:

$$\frac{1}{v} \frac{\partial}{\partial t} \phi(r, \Omega, E, t) = -\Omega \cdot \nabla \phi(r, \Omega, E, t) + S(r, \Omega, E, t) - \Sigma_t(r, E, t) \phi(r, \Omega, E, t) + \int_0^\infty dE' \int_{4\pi} d\Omega' \Sigma_s(r, E' \rightarrow E, \Omega' \rightarrow \Omega, t) \phi(r, \Omega, E, t) \quad (3.2)$$

Where

$\phi(r, \Omega, E, t)$  = the expected number of particles per unit time at  $r$  with energies in unit energy about  $E$  and moving in a unit angle about  $\Omega$ ,

$S(r, \Omega, E, t)$  = the number of source particles emitted in a volume  $dV$  travelling in a cone of direction  $d\Omega$  about  $\Omega$  with energies between  $E$  and  $dE$

$\Sigma_s(r, E' \rightarrow E, \Omega' \rightarrow \Omega, t)$  = macroscopic scattering cross-section which is the probability that the particles at position  $r$  with energy  $E'$  travelling in the direction  $\Omega'$  scatter into  $dE$  about  $E$  and into the cone of direction  $d\Omega$  about  $\Omega$

The corresponding steady state equation is

$$[\Omega \cdot \nabla + \Sigma_t] \phi(r, \Omega, E) = \int dE' \Sigma_s(r, \Omega' \rightarrow \Omega, E' \rightarrow E) \phi(r, \Omega', E') d\Omega' dE' + S(r, \Omega, E) \quad (3.3)$$

The neutron transport equation holds under some strict assumptions such as (Miller & Lewis, 1993):

- The particles are treated as points.
- Between any two points, particle motion is in straight line.
- Interactions between particles are not considered.
- Collisions are prompt.
- Isotropic properties are assumed for the material.

- Material composition and nuclei properties are known and time dependent.
- The particle density distribution is the mean value.

### **3.4 Methods Used to Solve or Simulate Neutron Transport**

There are several computational codes available for use in light water reactor analysis based on either deterministic methods or Monte Carlo methods.

#### **3.4.1 Deterministic Methods**

Deterministic methods basically solve the neutron transport equation for the average particle behaviour. A deterministic model has no stochastic elements and the entire input and output relation of the model is decisively determined. The discrete ordinate method sees the geometry or phase space to be divided into many volumes and angles. The neutron transport equation is then solved in terms of the volumes and discrete angles. If this method is used to model the HPR or EPR core, the moderator, fuel rods, guide tubes and instrumentation tubes will be homogenised for each volume and angle to be able to solve the transport equation.

Examples of these codes are Discrete ordinate transport code DORT, TORT and DORT-TD. DORT is a one and two-dimensional (1D and 2D) code while TORT is a two and three-dimensional (2D and 3D) discrete transport code (Pautz, 2005) and DORT-TD is a transient neutron transport code (Waata, 2006).

### 3.4.2 Stochastic Methods (Monte Carlo Method)

Stochastic methods or Monte Carlo do not solve the transport equation like the deterministic method based codes mentioned above, but rather simulates particle transport for each particle by tracking the path of each individual particle throughout its life time and records (tallies) the average behaviour of these particles.

In Monte Carlo method, each individual particle is simulated and their behavior recorded. For every probabilistic event, there is a probability distribution that governs it. These distributions are statistically sampled to determine their average behavior and the total phenomenon (Staff, Los Alamos National Laboratory, 2008). These statistical sampling process is based on selecting a random numbers, like throwing dice in a casino, thus the name “Monte Carlo.” A large number of particle simulations (trials or histories) are required to accurately describe the phenomenon. Each of the particles is tracked throughout its life from source to death. Probability distributions are arbitrarily inspected utilizing transport information to decide the result at each progression of the reenacted molecule's life. Monte Carlo (MC) techniques, contrasted with deterministic strategies, are appropriate for complex three-dimensional, time dependent problems. MC strategies permit correct geometry details. However, deterministic methods solve the transport equation for discrete units and uses averaging approximations for space, time and energy. In addition, MCNP uses point-wise (continuous) cross sections. Point-wise cross sections follow the true cross sections as a function of energy, but calculations using point-wise cross sections can be computationally expensive. Cross sections represent the area a nucleus presents to an incident particle of a specific energy and type. Cross sections for most nuclides are included in libraries used by MCNP. Deterministic methods require group-wise cross sections,

which are based on energy groups. Group-wise cross sections are created from collapsed/averaged continuous cross section libraries. While group-wise cross sections allow faster calculations, calculations using group-wise cross sections are not as accurate as calculations using point-wise cross-sections. Geometries are created in MCNP by specifying surfaces that define the boundaries of volumes called cells. Cell characteristics such as temperature, material, density, and particle importance are specified, and materials are defined by their constituent nuclides and respective mass or atom fraction. An appropriate cross section library is specified for each nuclide. To verify and easily locate geometry errors visually, the Visual Editor (VISED) program can be used. VISED reads the MCNP input file and runs on MCNPX.

### 3.5 Isotopic Depletion

The exposure of an isotope  ${}^A_ZX$  to neutron flux produces nuclear reactions that may modify its nuclear characteristics. Such reactions basically are of ; fissions, neutron capture, radioactive disintegrations and (n, 2n) reactions.

- ❖ Radiative capture (n,  $\gamma$ )  ${}^A_ZX + {}^1_0n \rightarrow {}^{A+1}_Z X$
- ❖ Fission (n, f)  ${}^A_ZX + {}^1_0n \rightarrow C_D Y + {}^{A+1-C-V}_{Z-d} Z + v {}^1_0n$
- ❖ (n, xn) reaction)  ${}^A_ZX + {}^1_0n \rightarrow {}^{A+1-x}_Z X + x {}^1_0n$
- ❖ (n,  $\alpha$ ) transmutation  ${}^A_ZX + {}^1_0n \rightarrow {}^{A-3}_{Z-2} Y + {}^4_2\text{He}$
- ❖ (n, p) transmutation  ${}^A_ZX + {}^1_0n \rightarrow {}^A_{Z-1} Y + {}^1_1\text{H}$

In each burnup mixture of the unit cell, the depletion of i isotopes over a time stage follows the following equation :

$$\frac{dN_i}{dt} = \underbrace{-\sigma_i^{\text{abs}} \Phi N_i + \sum_{j \neq i} \sigma_{j \rightarrow i} \Phi N_j}_{\text{Reaction}} - \underbrace{\lambda_i N_i + \sum_j \lambda_{j \rightarrow i} N_j}_{\text{Decay}} \quad (3.2)$$

Where  $N_i$  = the number of nuclei for isotope  $i$ .

$\sigma_i^{\text{abs}} \Phi$  = the average reaction rate of absorption of the nuclei  $i$ .

$\Phi \sigma_{j \rightarrow i}$  = the average rate of reaction of the nuclei  $j$  of the reaction producing  $i$ .

$\lambda_i$  = the total decay constant of nuclei  $i$ .

$\lambda_{j \rightarrow i}$  Is the decay constant of nuclei  $j$  to produce nuclei  $i$  (Sogbadji, David, Akaho, & Nyarko, 2016).

Harry Bateman was the first to present a general analytical solution for a linear chain of decay reactions. Therefore, this system of linear first order differential equations was named after him and called Bateman equations.

The first two terms define the neutron reactions, capture and fission. And the last two represents the natural decay of the nuclei.

To solve this equations, a matrix of evolution have to be defined for each evolving isotope. Simulating the evolution of the nuclear fuel involves solving digitally the Bateman equations system in each evolving isotope (Sogbadji, David, Akaho, & Nyarko, 2016). In this study MCNPX code was used to achieve this. MCNPX is CINDER integrated for fuel depletion and burnup calculations. CINDER'90 is described in the next section.

### 3.6 CINDER'90

CINDER'90 is a computer code used to calculate the nuclide inventory of irradiated materials.

CINDER'90 has an inbuilt file i.e cinder.dat which contains library to calculate different parameters for a radionuclide, such as, activity density, the atomic density, delayed-neutron production rate, and spontaneous fission, absorption, decay and neutron fission reactions of every nuclide at a specified time.

The code tracked the burnup of fissionable material and also the production of fission products.

CINDER'90 has a pre-generated library of 63-group neutron cross sections. The cross-section data in the CINDER'90's cross section data comes from libraries ENDF-B, JEF, JENDL, and evaluation codes such as GNASH (Fensin M. L., 2008).

The library of CINDER'90 currently covers 3,400 nuclides that range between an atomic number,  $Z$ , of 1 and 103 (Wilson, 2008). The code requires multigroup neutron flux for neutron energies less than 20 MeV and nuclide production rates for reactions at higher neutron energies or for additional particles (Wilson, 2008).

#### 3.6.1 CINDER Atom Density Algorithm (Markovian Chains)

A Nuclide is a specie of atom defined by the number of protons, neutrons, and energy content in the nucleus, i.e. by the atomic number, mass number, and atomic mass. (Wilson, 2008).

The differential equation describing the rate of change in the atom density,  $N_m(t)$ , of nuclide  $m$  is constructed as the sum of the rates of losses and gains in nuclide density

(Wilson, 2008). The loss term is due to transmutation, radioactive decay, and particle absorption reactions producing daughter and product nuclides that are different than the original nuclide  $m$ . Gains are from transmutation of other nuclides with nuclide  $m$  as a daughter or reaction product. For some applications, an additional constant production rate  $\bar{Y}_m$ , can be included accounting for production beyond the energy and particle domain of the CINDER'90 nuclear data library (Wilson, 2008). The atom density differential equation is shown in equation below.

$$\frac{dN_m(t)}{dt} = -N_m(t)\beta_m + \bar{Y}_m + \sum_{k \neq m} N_K(t)\gamma_{K \rightarrow m} \quad (3.3)$$

Where  $\beta_m$  is the total transmutation probability of nuclide  $m$ , and  $\gamma_{K \rightarrow m}$  is the probability of nuclide  $k$  transmuting by decay or absorption to nuclide  $m$ .

$$\beta_m = \lambda^m + \phi \sigma_a^m \quad (3.4)$$

Where  $\phi$  = the energy integrated neutron flux.  $\lambda^m$  = the total decay constant of nuclide  $m$ , and  $\sigma_a^m$  = the flux weighted average cross section for neutron absorption by nuclide  $m$ . Absorption reactions of  $\sigma_a^m$  are all of those with products other than nuclide  $m$ . This includes inelastic scattering to states other than that of nuclide  $m$  (Wilson, 2008). Equation 3.3 is nonlinear because the transmutation probabilities depend on time integrated flux, which is also dependent on time integrated atomic density. To make the process linear, it is assumed that the transmutation probabilities  $\beta_m$  and  $\gamma_{K \rightarrow m}$  are constant. Thus, the flux is assumed to be constant for the duration at which the solution is calculated. Since the flux is dependent on the nuclide inventory, time intervals are selected based on the time frame of the production of nuclides. The selected time interval is set in the MCNP input file which is discussed further in chapter four. The set of differential equations that describes all

nuclides are coupled. The equations are coupled because each equation is interrelated and contains atom density information of other nuclides. This set of coupled differential equations is reduced to a set of independent, linear differential equations using the Markov method (Wilson, 2008). The Markov method makes it possible to create linear chains for each nuclide transmutation path, beginning from an the first specified nuclide concentrations (Hendricks, 2008). Equation 3.5 is generated from the linear chains for all nuclides.

$$\frac{dN_i}{dt} = -N_i(t)\beta_i + \bar{Y}_i + N_{i-1}(t)\gamma_{i-1} \quad (3.5)$$

Where  $\gamma_{i-1}$  = the probability of transmutation for forming nuclide  $i$ . The quantities are listed in the order in which they appear within a given linear chain. Therefore, the differential equation governing the computation of nuclide with time(t) is only linked to any preceding elements in the linear chain, whose parameters are known and solutions obtained, leading to the  $i^{th}$  element. The solution of each linear chain determines a partial nuclide density,  $N_i$  which is now integrated to determine the total nuclide inventory of nuclide  $N_m$ . The general solution for a linear chain of nuclides related by any sequence of radioactive decay or particle absorption is shown by equation 3.6 (Hendricks, 2008).

$$N_n(t) = \sum_{m=1}^n \left\{ \prod_{k=m}^{n-1} \gamma_k \right\} \left( \bar{Y}_m \left[ \frac{1}{\prod_{l=m}^n \beta_l} - \sum_{j=m}^n \frac{e^{-\beta_j t}}{\beta_j \prod_{l=m, l \neq j}^n (\beta_l - \beta_j)} \right] \right) + N_m^0 \sum_{j=m}^n \frac{e^{-\beta_j t}}{\prod_{l=m, l \neq j}^n (\beta_l - \beta_j)} \quad (3.6)$$

This procedure promulgates the initial nuclide densities and constant production rates of all nuclides  $m=1, n$  to the present density  $N_n$  of the  $n^{th}$  nuclide in the sequence (Waata, 2006). CINDER'90 does not require any pre-determined sequence of nuclides to provide the nuclide inventory. All production paths available by the nuclear data libraries are

followed until found irrelevant or inaccurate. A quantity called passby ( $P_n$ ) is used by CINDER'90 to enumerate the transmutation of nuclide  $n$  and determine the significant elements of the path. The passby is the number of atoms of nuclide  $n$  transmuted during the time step and is given by equation 3.7.

$$p_n(t) = \beta_n \int_0^t N_n(t') dt' \quad (3.7)$$

The limiting passby value is defined in the user input and determines if a sequence will be terminated. This value will be discussed with the BURN card in chapter four.

### 3.7 MCNPX/CINDER'90

MCNPX is a Monte Carlo based transport code. MCNPX and CINDER'90 have been internally coupled for fuel depletion and burnup calculations. MCNPX version 2.7.0 was used for this study. The depletion calculation is a coupled process that involves flux calculations in MCNPX and nuclide depletion calculations in CINDER'90. MCNPX does steady-state calculations which provides 63-group fluxes, the system eigenvalue ( $K_{eff}$ ), fission multiplicity ( $\nu$ ), energy-integrated reaction rates, and recoverable energy per fission ( $Q$  values) for a given time step. The MCNPX results are then transferred to CINDER90. CINDER'90 does the depletion calculations and generates new number densities corresponding to the inventory at the end of the time step. The new number densities are inserted into MCNPX which produces a new set of fluxes and reaction rates for the updated nuclide inventory. This process is repeated as defined by the user. MCNPX calculates the parameters based on : 1. The listed materials in the material cards section of MCNPX 2. The nuclides produced by the nuclide generator algorithm or selected by the specified fission product tier (Hendricks, 2008). The material cards are modified and updated by

CINDER'90. CINDER'90 tracks the time-dependent reactions for 3,400 nuclides, for which there are inherent data libraries. MCNPX can only track energy integrated reaction rate information for nuclides that MCNPX has transport cross sections for. MCNPX does not have transport cross sections for the same 3,400 nuclides that CINDER'90 tracks, therefore it does not include all of the nuclides from CINDER'90 into the transport calculations. MCNPX takes the 3,400 nuclides output from CINDER'90 and reduces the nuclides tracked to those described earlier i.e. nuclides originally listed in the material cards, immediate daughter and decay products, and fission products. For nuclides whose transport cross-section information is not present in MCNPX, MCNPX calculates a 63 group flux that is sent to CINDER'90. This MCNPX generated flux spectrum is matched with a 63 group cross-section set in CINDER'90 to generate the 63 group reaction rates. These 63 group reaction rates are then integrated with respect to energy to determine the total reactions and transmutation unfolding. MCNPX assumes a constant flux throughout the burn step. This will enable the nuclide density calculations to be linear. In reality, the flux and nuclide inventory influence each other. So MCNPX uses a Predictor-Corrector technique to improve the accuracy. This technique is a multistep process, as shown in Figure 3.1.

1. in CINDER90, burnup calculation is completed to the half time step called the predictor step  $[t(i) \rightarrow t(i+1/2)]$
2. collision densities and fluxes are calculated again in a steady state MCNPX calculation at the half-time step.

- The re-calculated collision densities and fluxes are now used to burn over the full time step known as corrector step.  $[t(i) \rightarrow t(i+1)]$ .

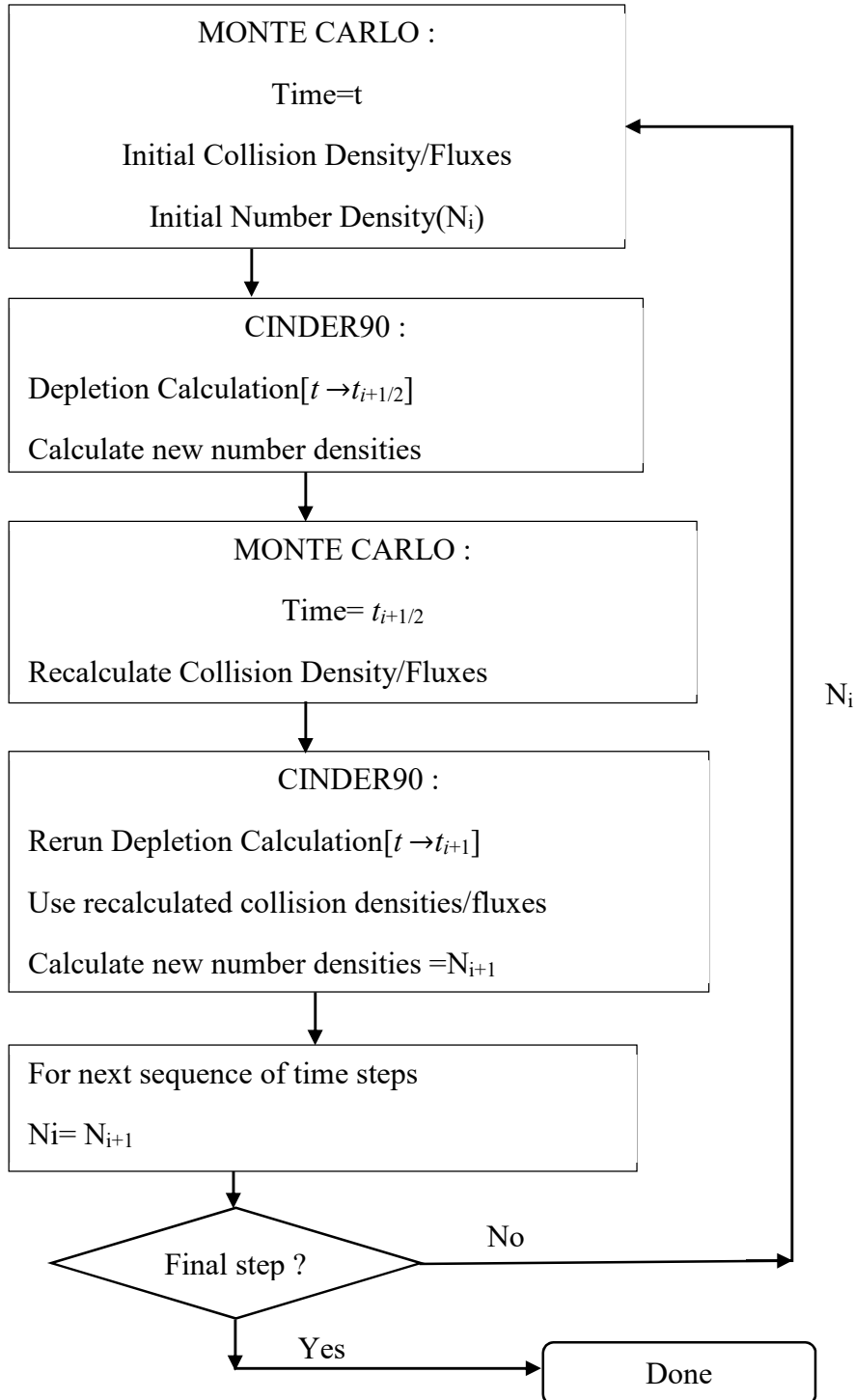


**Figure 3.1 : MCNPX & CINDER'90 Predictor Corrector Method**

The fluxes and reaction rates calculated at the corrector step are assumed to be the average fluxes and reaction rates experienced during the entire time step. This is true if the change in flux is linear between the beginning and end of the time step. This technique allows longer burn steps than if no approximations were made for the flux. Burn calculations are computationally expensive, so reducing the required steps decreases computer resource demand. Although the Predictor-Corrector approach increases accuracy, large burn steps that experience large flux shape changes will result in inaccurate calculations during the time step. Time steps chosen are defined in the BURN card section in chapter four.

### **3.8 Radiotoxicity**

When a human being ingest a radioactive material, the radioactivity he or she is subjected to is inadequate in quantifying the risk to the human being, thus the concept of radiotoxicity by ingestion was developed. Radiotoxicity by ingestion (which is applied in this study) succinctly quantifies the radiological hazard to human being from ingestion of a radioactive material.

The ecological danger of the various available nuclear fuel cycles arises from the radiotoxicity of long-lived radioactive wastes, present in the spent nuclear fuel coming from these nuclear fuel cycles. The radiotoxicity of a radioisotope is influenced by the following factors ; 1. The energy of its radiation 2. Body tissue where it is absorbed in the organism, 3. total time of irradiation in the body. For the radiotoxicity( $Sv$ ) analyses of each radionuclide, the contribution dose is proportional to the total activity  $A$  (in Bq), where the dose coefficient is called the Dose conversion Factor ( $F_d$ ). It could be via ingestion or by inhalation (in  $Sv/Bq$ ).

$$R(Sv) = F(Sv/Bq) \times A(Bq) \quad (3.12)$$

The radiotoxicity of each nuclide varies with time as :

$$R_i(t) = F(i) \times \lambda_i N_i(t) \quad (3.13)$$

Where  $N_i$  is the quantity of nuclide present in isotope,  $i$ , at time  $t$ .

From the above equation, it can be seen that radiotoxicity is a function of the activity  $A$  and dose factor  $f$ . Thus, the total radiotoxicity from the different nuclei  $i$  in  $Sv$  is expressed as:

$$R(t) = \sum_i f_i \lambda_i N_i(t) \quad (3.14)$$

Where  $f_i$  = the factor dose of the nuclei  $i$ ,  $\lambda_i$  = the decay constant of the nucleus  $i$ , and

$N_i(t)$  = the number of nuclei  $i$ .

Futhermore, the dose factor is represented as ;

$$f_i = h_{E,50} = \sum_T W_T h_{T,50} \quad (3.15)$$

Where ;

- $h_{E,50}$  = The effective dose equivalent conversion factor (expressed in Sv/Bq), i.e., the committed effective dose equivalent per unit intake of radionuclide
- $h_{T,50}$  = The tissue dose equivalent conversion factor for organ or tissue T (expressed in Sv/Bq), i.e., the committed dose equivalent per unit intake of radionuclide.
- $W_T$  = weighing factor for the tissue (Eckerman, Wolbarst, & Richardson, 1987)

Most of the time radiotoxicity by ingestion is used in waste characterization in a geological storage. This is because radionuclides will only pose a risk once it could migrate from the disposal towards the biosphere where there's possibility of ingestion. (Sogbadji, David, Akaho, & Nyarko, 2016).

The next chapter describes the MCNPX input deck geometry setup as well as the BURN card setup that was used to simulate depletion of the nuclear fuel assembly for the two reactors under consideration.

## CHAPTER FOUR

### 4.0 METHODOLOGY

#### 4.1 Introduction

In this chapter, the 3-D Monte Carlo input deck created for the reactors using the MCNPX code is described. The burn card setup which MCNPX requires to perform depletion calculations is described. The methodology adopted in determining the radiotoxicity is also described.

#### 4.2 MCNPX

MCNPX is a computer software code used to simulate neutron, photon, electron transport and radioactive particles reactions while treating an arbitrary three-dimensional configuration of material in a geometry of a system, taking into consideration the point wise continuous energy cross section libraries that represent nuclear reactions in the  $10^{-11}$  to 20 MeV energy range.

MCNPX also has the capability to simulate fuel burnup and depletion to provide the radionuclide content as a result of fission for all fissionable and fissile isotopes and also calculating the decay of parent nuclides. MCNPX is internally coupled with the CINDER code which makes burnup simulation possible. The cinder.dat file allows the transfer of one-group reaction rates (cross-sections) and 63 group neutron fluxes to the depletion code CINDER for decay calculations.

In this study, MCNPX version 2.7 (with ENDF/B-VII.1, ENDF/B-VII.0, older data libraries, and thermal neutron scattering libraries) was used.

### **4.3 MCNPX Model of the Reactors**

In order to build a representative MCNPX model of the respective reactors, an input file was created. The MCNPX models of the reactors described below cover all important details of their fuel assembly designs. The model was built as precisely to the design specifications as possible, with inherent MCNPX geometric modelling inadequacies introduced in the process. The model description and assumptions are discussed in the ensuing sections.

The following assumptions were made in developing the model:

- ❖ Steady state
- ❖ No temperature feedbacks
- ❖ No xenon
- ❖ Boron concentration 1383 ppm
- ❖ The assembly side boundaries are periodic for infinite assembly models

The EPR and HPR have very similar geometry and their MCNPX input model is discussed in the next section.

#### **4.3.1 HPR and EPR Models**

The EPR and HPR fuel assemblies are both designed to have a square lattice containing 265 fuel pins. However, small differences exist in terms of the dimension of the fuel meat diameters. The Lattice (lat1 for square array) and Fill cards of the MCNPX are used to design the square lattice of the HPR input file to contain 265 fuel pins. Fuel enrichment of 1.8% is used for the HPR fuel pins which is the minimum enrichment for HPR fresh core. Light water with a density of 0.98g/cc is used as moderator and coolant.

Similar approach was adopted in designing the input file for the EPR using the Lattice (lat1) and Fill cards of the MCNPX to model the square lattice containing the 265 fuel pins. The fuel pins are surrounded by the light water moderator and coolant also with a density of 0.98 g/cc. Fuel enrichment of 1.4% is used for the EPR fuel pins which is the minimum enrichment for EPR fresh core. The cell card and surface card is used for this geometry modelling. The design parameters of the HPR and EPR model used in designing the MCNP input file are presented in Table 4.1 below.

**Table 4. 1 Fuel Assemblies Design Specifications**

PARAMETERS	DIMENSIONS (mm)	
	EPR	HPR
Fuel pin diameter	9.5	9.5
Cladding thickness	1.14	1.14
Gap	0.16	0.168
Fuel part diameter	8.2	8.192
Step between rods	12.6	12.6
Length of active height	4199.99	3658
Number of fuel rods	265	265

The MCNP geometry plot card is used to view the geometry modelled for the HPR and EPR and the pictorial view presented in the figures below.

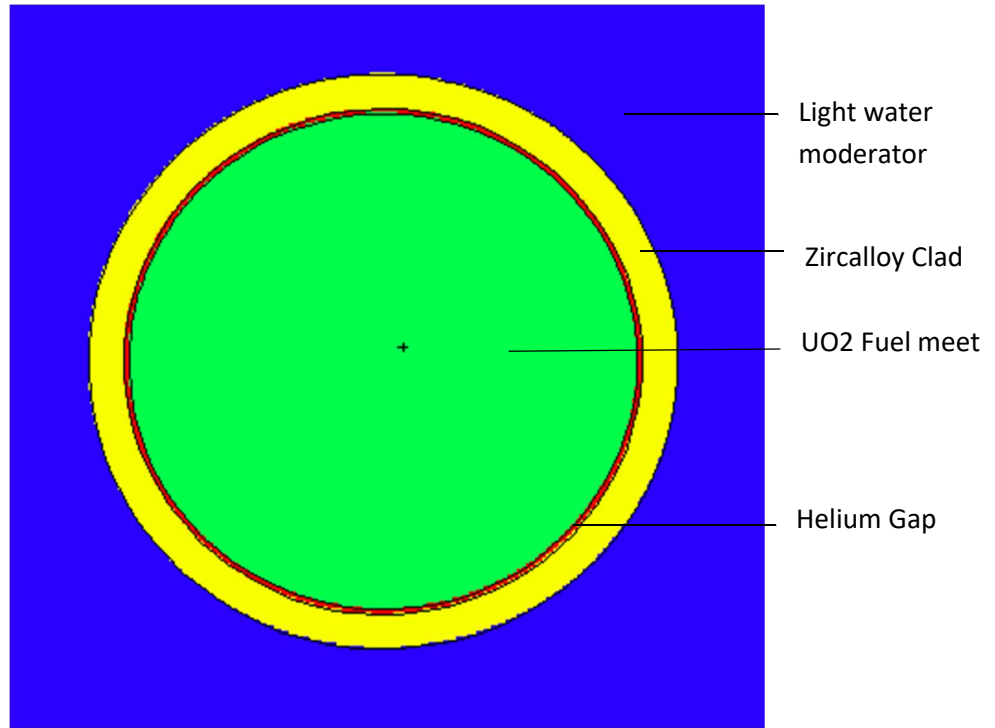


**Figure 4. 1 MCNPX Plot of Transverse Section of HPR Fuel Pin**

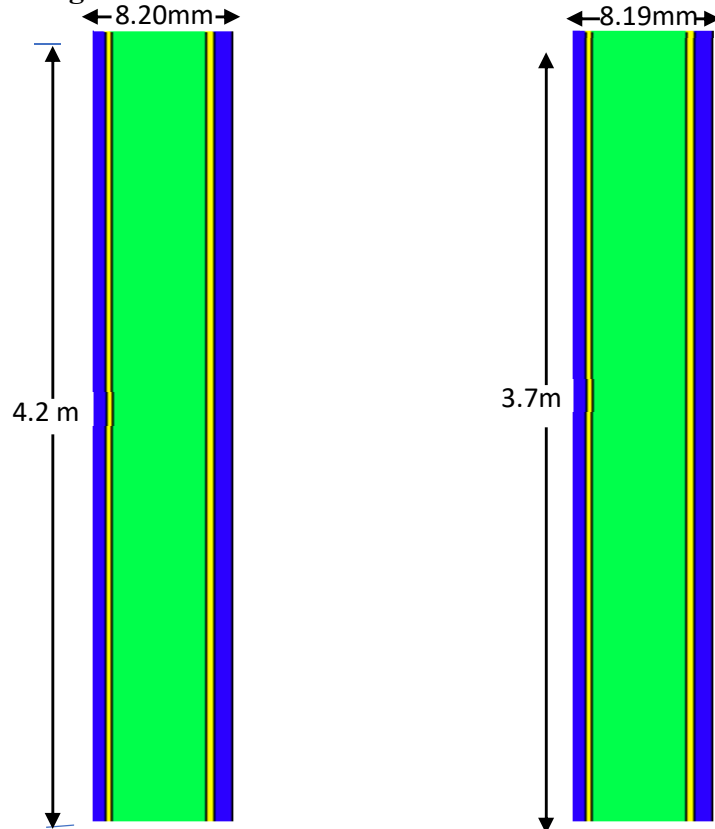


**Figure 4. 2 MCNPX Plot of Longitudinal Section of the EPR and HPR Fuel Pin  
Respectively**

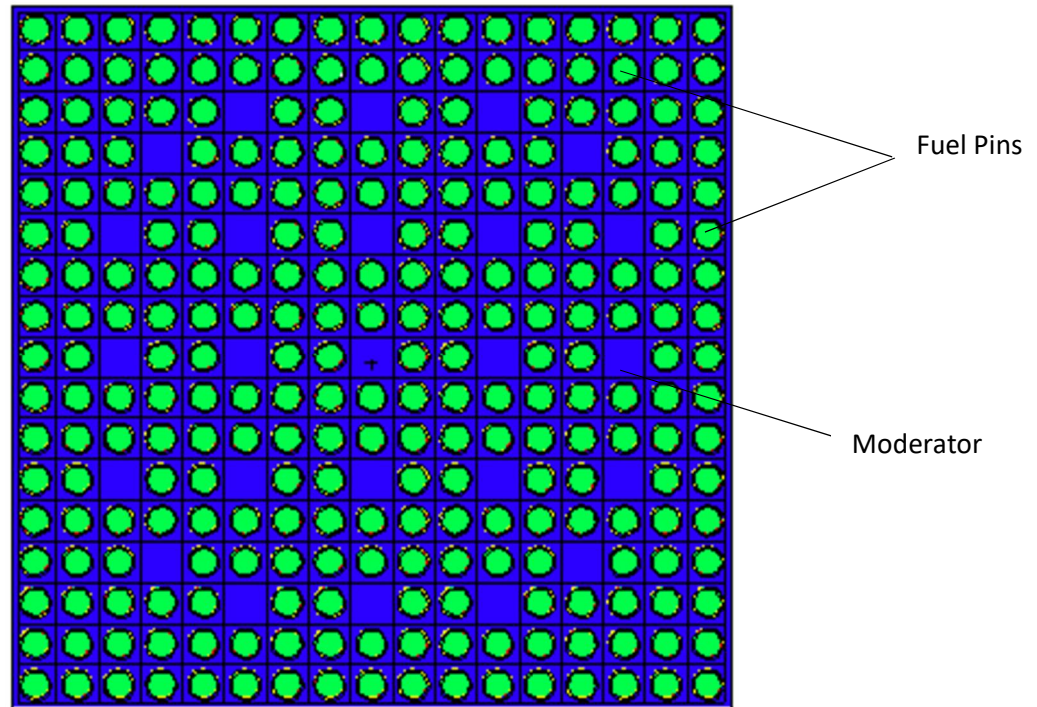


**Figure 4. 3 MCNPX Plot of Transverse Section HPR Fuel Assembly**

#### **4.4 Source Parameters**

For burnup and depletion calculations, MCNPX presently works only with criticality situations. The criticality of the two reactor types is calculated using the KCODE and SDEF card. A uniform neutron source is created using the SDEF card and the initial point of fission in the fuel meat specified at the point 0,0,0 (x,y,z) on the fuel pin. The specifications on the KCODE card is vital for criticality calculations so that MCNPX can exhibit a small bias in the calculated  $k_{\text{eff}}$ . The larger the number of  $k_{\text{eff}}$  cycles used, the smaller the bias. 100,000 neutrons per cycle is used in this case. 200 active  $k_{\text{eff}}$  cycles was run which is a large enough number to ensure the system behave normally and fission source is converged. 85  $k_{\text{eff}}$  cycles was skipped to enable the calculated spatial fission source to converge to the fundamental mode. The MCNPX makes use of three different estimates

(i.e absorption, collision and scattering) statistically combined, in computing the  $k_{\text{eff}}$  value used in this study. The KCODE and the SDEF card are the control cards used.

The criticality was run and the SRCTP file generated. This file contains fission points information from the criticality simulation that was run. The best initial source distribution is from an SRCTP file from a previous calculation of a similar system (Hendricks, 2008). The SRCTP file is used in this study for the burnup simulation together with the burn card incorporated into the input deck for both reactors considered.

#### **4.4 Material Specification**

Nuclear data were obtained from the ENDF/B-VII nuclear data libraries for fissionable and fissile isotopes present in the materials which includes the clad, coolant, fuel meat and the moderator. The special  $S(\alpha,\beta)$  scattering feature was applied in the nuclear model to treat thermal scattering in hydrogen in light water for the water regions of the reactor models. Since the thermal hydraulic calculations were not performed, the temperatures of all the material at normal operation conditions were taken to be 300°C and the density of the moderator was taken to be 0.98 gcm<sup>-3</sup>.

#### **4.5 Burn Card Setup**

This section discusses the BURN card setup and the individual parameters chosen. In MCNPX, the depletion and Burnup calculation is a linked process. MCNPX first runs steady state calculations to determine the system's  $k_{\text{eff}}$ , energy integrated reaction rates, fluxes, fission multiplicity and recoverable energy per fission. CINDER now uses these results to perform burnup and generate new number densities for the next time step. To perform these, a BURN card is set up in the input deck.

#### **4.5.1 TIME**

The TIME card was used to define the duration, in days, of the burn step. 360 days core lifetime was used in this study with average burn step of 30 days. In other to ensure that the reactor performs effectively, it is a practice to remove about one-third of the spent fuel every one year or 18 months and replacing it with fresh fuel (World Nuclear Association, 2017).

#### **4.5.2 POWER**

The POWER card was used to specify the thermal power level, in MW, of the reactor. On the POWER card, 17.1 for HPR and 18.1MW for EPR (average power per assembly) which corresponds to total thermal power of 3000MW and 4500MW in 177 and 241 assemblies respectively was used.

#### **4.5.3 PFRAC**

The PFRAC card was used to specify the power fraction of each time step. PFRAC of 0.25 was chosen for each burn step. The PFRAC was set to zero for the decay calculations for the time steps of 365,3285,32850,328500,3285000,32850000,328500000 days to calculate radionuclide decay for the next 1, 10,100, 1000, 10000, 100000 and 1000000 years in SNF storage.

#### **4.5.4 MAT**

The MAT card was used to set the material number burned as defined in the material card of the MCNPX input file, which in this case is the UOX fuel meat.

#### **4.5.5 OMIT**

The OMIT was used to omit Xenon 135 from the transport calculation. This was done to remove the reactivity changes that Xe-135 is known to cause due to its large neutron absorption cross section. Although negative reactivity coefficient of xenon 135 was not performed in this study, it was assumed that the negative reactivity coefficient could cause reactivity changes.

#### **4.5.6 AFMIN**

The AFMIN card was used to define the minimum atom fraction tracked by CINDER. AFMIN value of E-32 was used to accommodate large enough atom fractions from different nuclides to be tracked by CINDER.

#### **4.5.7 BOPT**

The BOPT card contained three input i.e. B1, B2, and B3. The B1 is the Q value multiplier ; its default value of 1 was used in this study. The parameter B2 is used to control the ordering and content of the CINDER output. B2 value of -24 was used to organise the output by increasing Z, and tracks all nuclides contained in the fission product array in current cross section directory (i.e. XSDIR). It also generates output after each burnstep completed. In this study, B3 default value of 1 is used which allows MCNP to run with models i.e. it will use cross-section models for isotopes not containing tabular data.

#### 4.6 Radiotoxicity

The radiotoxicity was calculated as ;

$$R(\text{Sv}) = F(\text{Sv/Bq}) \times A(\text{Bq}) \quad (4.1)$$

Where  $A(\text{Bq})$  is the activity value for each radionuclide calculated by MCNPX.

$F(\text{Sv/Bq})$  is the dose factor for the corresponding radionuclide as obtained in the ICRP 119 based on the compendium of dose coefficient on ICRP publication 60. In this study, dose factor due to ingestion was used.

The radiotoxicity values have been normalized to the thermal energy generated by the reactors for the one cycle of 12 months used. This was done by dividing the Radiotoxicity (Sv) per tonne of Uranium with the Burnup(MWd/t).

The reactor models were successfully developed and simulated to give desired results. The radiotoxicity was calculated and results are presented and discussed in the next chapter.

## CHAPTER FIVE

## 5.0 RESULTS AND DISCUSSION

## 5.1 Introduction

Radiotoxicity by ingestion helps to understand what comprise the hypothetic radiological risks to man of the nuclear elements generated during the operation of a nuclear reactor. The results in this study have therefore been presented in terms of the radiotoxicity by ingestion. Simply put, it is the 50 year committed dose for an adult after ingesting a radioactive element.

Radiotoxicity is expressed as ;

$$R(t) = \sum_i f_i \lambda_i N_i(t) \quad (5.1)$$

where  $f_i$  is the dose factor of the nuclei  $i$ ,  $N_i(t)$  is the number of nuclei  $i$  and  $\lambda_i$  the decay constant of the nuclei  $i$ .

$$f_i = h_{E,50} = \sum_T W_T h_{T,50} \quad (5.2)$$

where ;

- $h_{E,50}$  = The committed effective dose equivalent per unit intake of radionuclide
- $h_{T,50}$  = The tissue dose equivalent conversion factor for organ or tissue T (expressed in Sv/Bq), i.e., the committed equivalent dose per intake of radionuclide.
- $W_T$  = the weighing factor for the tissue (Eckerman, Wolbarst, & Richardson, 1987)

## 5.2 Nuclear Fuel Reactivity

The degree with which neutrons multiply in a reactor core is termed reactivity. This terminology directly relates to the tendency of the reactor core to change power level. Adjusting the reactivity can be achieved by control rods, when raised or lowered into the reactor core to obtain a desired power level change or to keep it constant. The density and temperature of the coolant or moderator, and the fuel temperature and density are also known to affect reactivity. The reactivity is evaluated as ;

$$\rho = \frac{K_{eff} - 1}{K_{eff}} \quad (5.3)$$

Where  $\rho$  is the reactivity and  $k_{eff}$  is the effective multiplication factor.

In measurements of fuel performance, the peak reactivity is key. This is because the higher the peak reactivity, the much higher the power output, since it has a direct proportionality on the power level. From the results, the calculated value of 0.271 and 0.29 was obtained for EPR and HPR respectively. This implies that the HPR nuclear fuel generated more power output than the EPR nuclear fuel.

## 5.3 The Effective Multiplication Factor

$$k_{eff} = \frac{\text{Neutron Produced from Fission in One Generation}}{\text{Neutron Produced from Fission in Preceding Generation}} \quad (5.4)$$

The effective multiplication factor's plot with time (i.e. at the beginning and end of core life) for the two reactors are as shown in Figure 5.1.

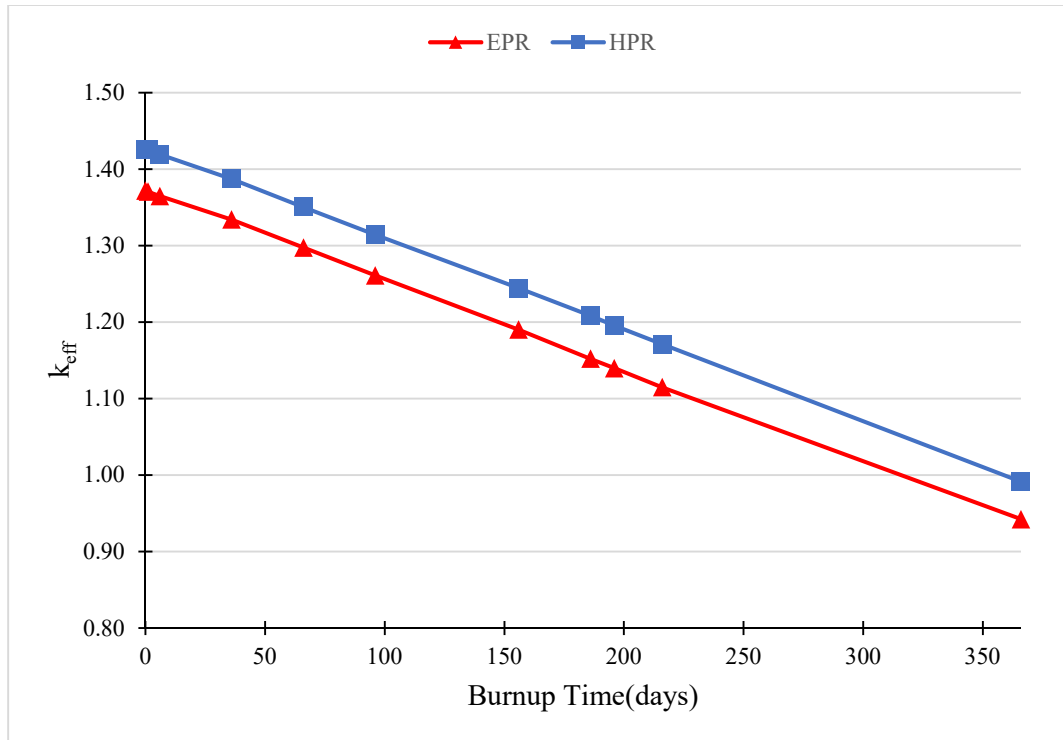


**Figure 5. 1  $k_{eff}$  Values against Burnup Time for EPR and HPR**

From Figure 5.1 it is noticed that the  $k_{eff}$  value drops for the UOX fuel of the two reactor types. This is as a result of neutrons being used up in fission of U-235 and also the neutron capture reactions by fissionable U-238 in the fuel. Also, fission products with high neutron absorption cross section absorbs neutrons thus reducing the neutron population. It is also noticed that the HPR fuel remains much critical for a higher part of the burnup period relative to EPR fuel. This is due primarily to the higher enrichment of HPR fuel compared to EPR, since both uses UOX fuel. It was also observed that the EPR fuel has gone subcritical before the 12 month while HPR fuel remained critical. This implies that HPR fuel produces more power for longer time than the EPR fuel before discharge.

### 5.4 BURNUP

The burnup values indicate the thermal energy released per metric ton of fissile uranium used up. Its value is proportional to the enrichment level used. The burnup is given in units of gigawatt days (GWD) per metric tons of uranium (MTU), where MTU is the sum of the masses of isotopes with protons  $\geq 90$ . Fig 5.2 shows the burnup profile for the reactors EPR and HPR. For the burnup simulation that was done, EPR reached a burnup of 47.58GWD/t while HPR reached a burnup of 56.19GWD/t, for the simulated period of one year. This characteristic of the HPR UOX fuel can be attributed to its higher fissile material content. More fission took place in the HPR UOX fuel thus improving the system power level. This constituted to the higher burnup value.

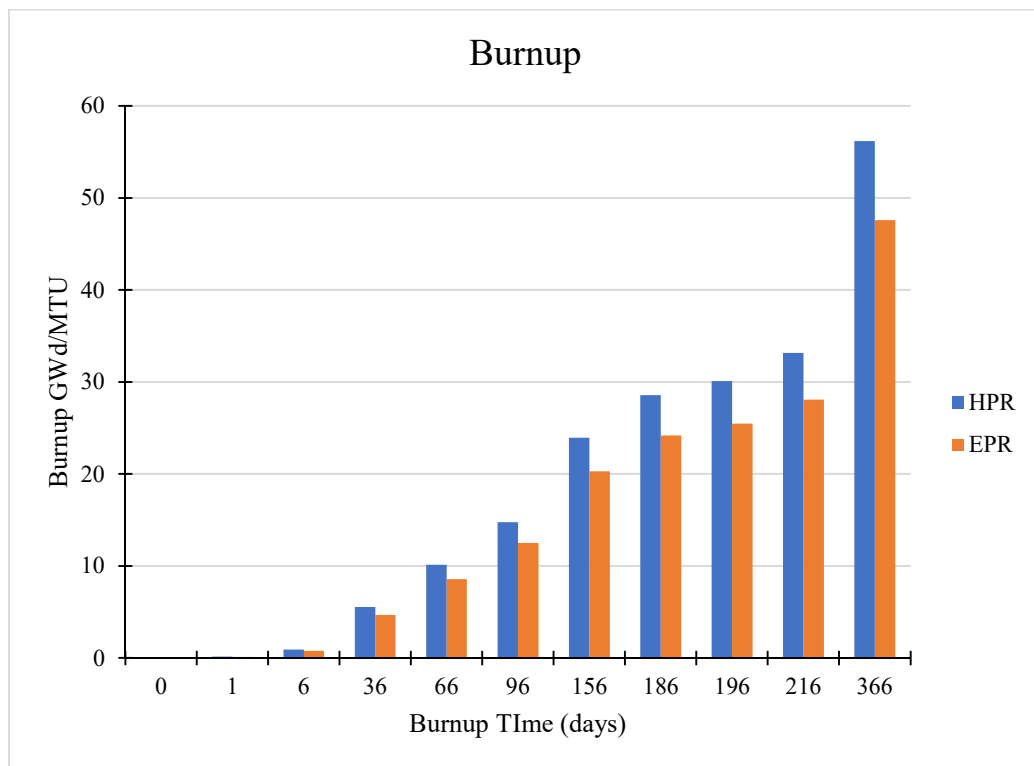


**Figure 5. 2 EPR and HPR Burnup Profile**

### 5.5 Time Evolution of the Major actinides in the EPR and HPR UOX fuel

The time evolution of the major actinides present in the EPR and HPR was examined to see how they vary with burnup. The results are as shown in Figures 5.3 to 5.5 for EPR and HPR.

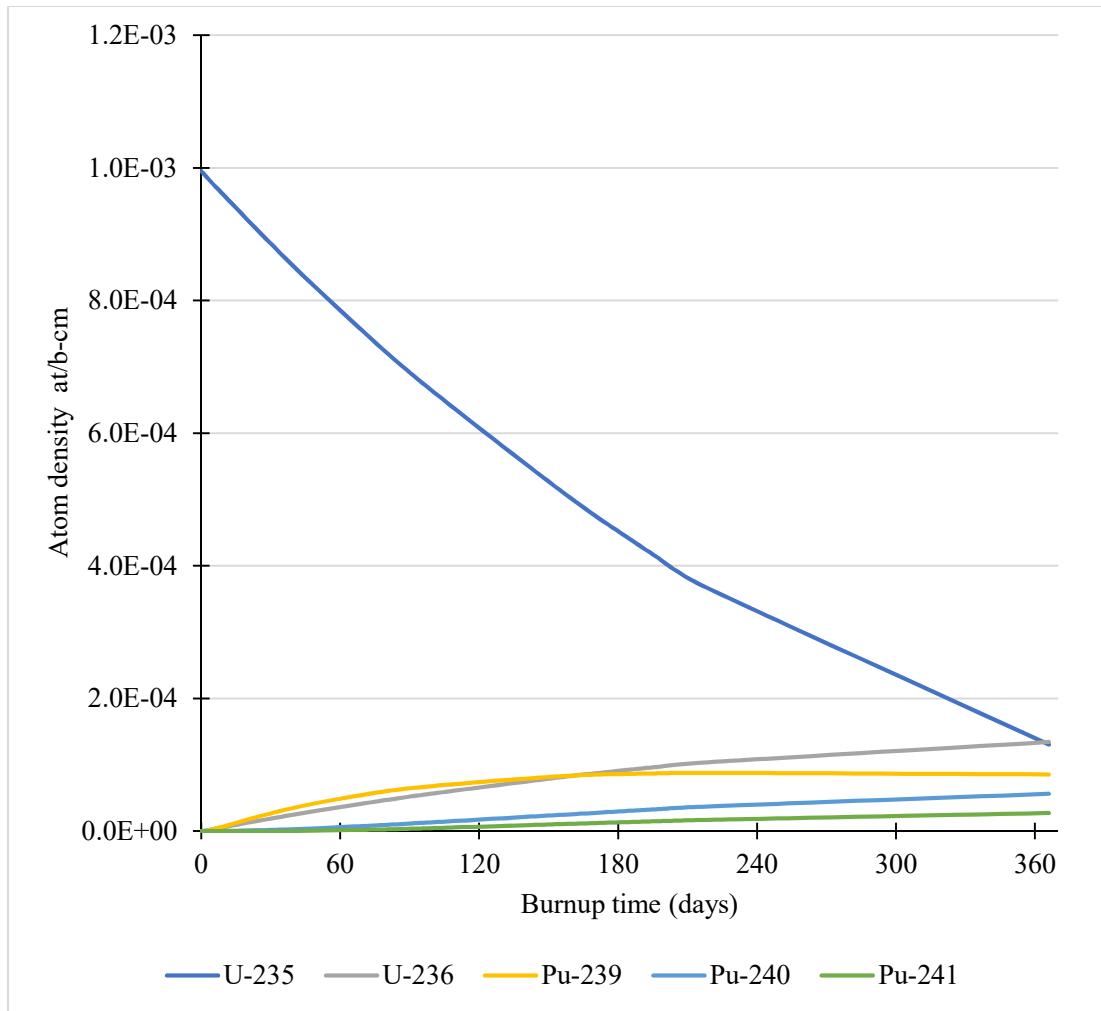


**Figure 5. 3 Atom density of the major Actinides with burnup time EPR**

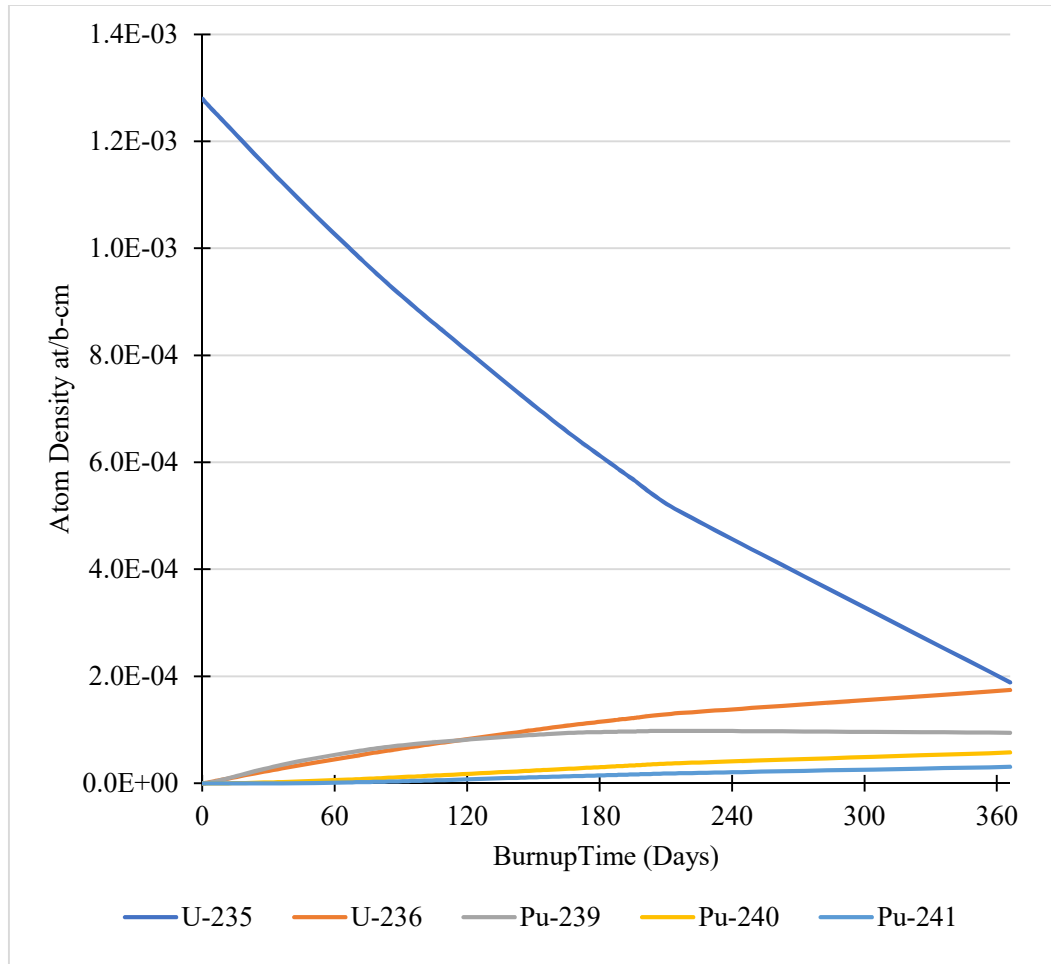


**Figure 5. 4 Atom density of the major Actinides with burnup time HPR**

It was observed that the uranium nuclide inventory varies similarly with burnup time for the two reactors SNF. U-235 decreases rapidly. This is because U-235 being fissile is being used up as fuel. U-236 radioisotope is observed to increase slightly with burnup. This is because U-236 is not fissile with thermal neutrons. They are generated mainly due to gamma radiation emission of U-235. Pu-240 isotope is observed to build up steadily for each of the two reactor fuels as it is formed occasionally by neutron capture process of Pu-239. It is also noticed that as burnup increases, Pu-239 atom density starts decreasing on the 216th day. This shows that Pu-239 is being used up in this period due to its ability

to fission with thermal neutrons. Another trend noticed is the build up of Pu-240 and Pu-241. This is due to the neutron capture reaction of Pu-239.

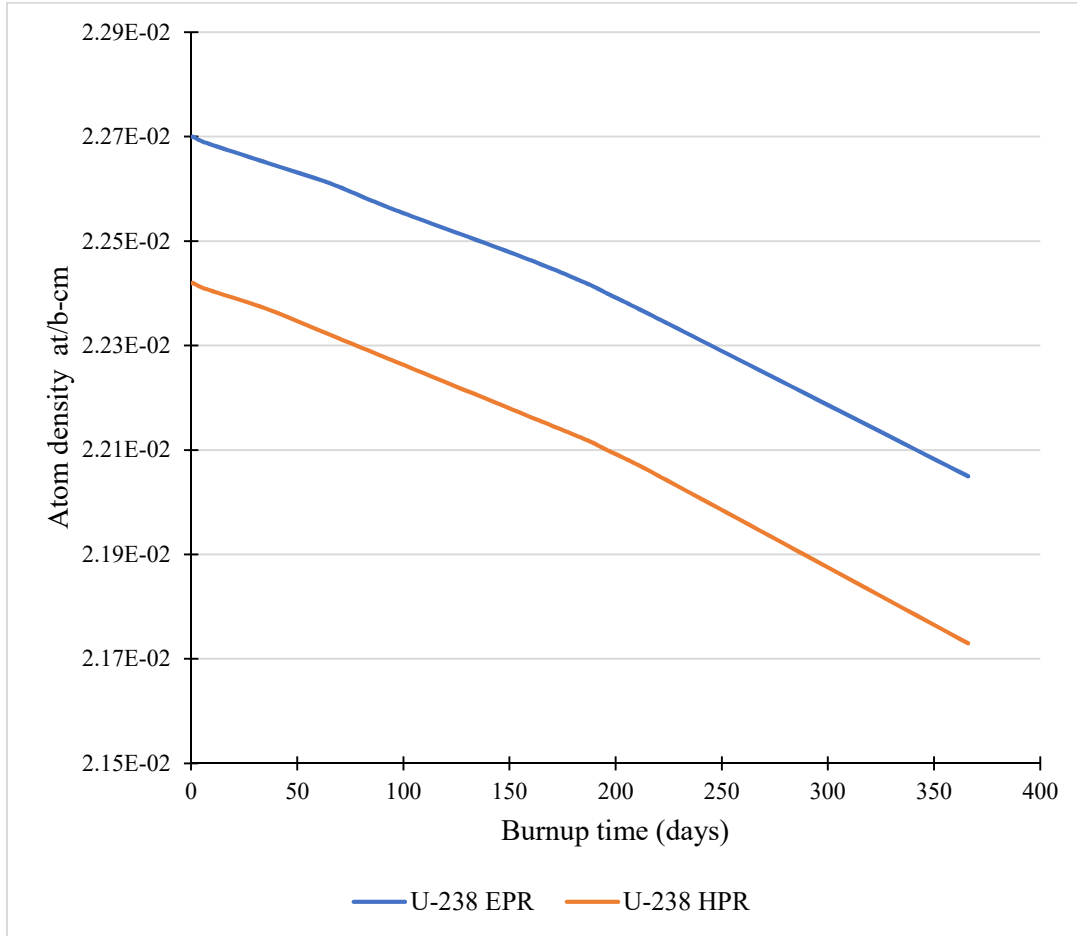
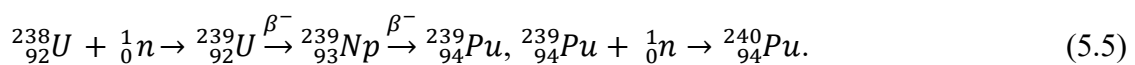


**Figure 5. 5 U-238 atom densities for EPR and HPR**

A slight steady decrease of U-238 is observed for the SNF of both EPR and HPR as shown in Figure 5.5 above. This is because U-238 being a fissionable material does not undergo fission with thermal neutrons but by its neutron capture reaction, it transmutes to Pu-239 which is fissile.



Boafo, et al., 2014, performed depletion analysis of an MNSR fuel using MCNPX. The trend obtained in this study shows similarity with the results from Figure 2.1 in the literature review.

## **5.6 RADIOTOXICITY**

The radiotoxicity of the UOX cycle for EPR and HPR considered in this work has been normalised to the thermal energy that the reactors generated (i.e. 47.58GWd/T for EPR and 56.19GWd/T for HPR) for one fuel cycle of 12 months. The major isotope's impact on the total ingestion radiotoxicity and approach to reduce the total ingestion radiotoxicity is discussed.

### **5.6.1 Radiotoxicity due to the Actinides and Fission product in the SNF**

The radiotoxicity contribution from the actinides and the fission products for the SNF for EPR and HPR are shown below in Figure 5.6 and Figure 5.7. It is observed that the initial high radiotoxicity of the SNF is from the fission products. This is as a result of the Cs-137 and Sr-90. The Cs-137 and Sr-90 can be removed by chemical reprocessing for their beneficial application in industry and nuclear medicine to reduce this initial high radiotoxicity. The characteristic radiotoxicity curve for the fission products is observed to steep downward due mainly to the decay of Cs-137, Sr-90 and other high radiotoxicity fission products in the spent fuel until around 1,000 years. When the initial high radiotoxicity has gone down due to the decay of the radionuclides causing it at about a thousand years, the radiotoxicity of the SNF from fission products till over a million years is now from the Tc-99 and I-129 due to their very long half lives.

The high radiotoxicity of the SNF above 100 years is from the Actinides when the Cs-137 and Sr-90 has decayed below this level as shown in the Figures. This dominance in radiotoxicity is from the plutonium isotopes. Reason for this is discussed in the proceeding sections. However, in order to reduce the overall radiotoxicity which is predominantly from the plutonium, the option of recycling can be adopted. The radiotoxicity curve of the actinides is also observed to decline with time. This is due to the eventual decay of the actinides mainly plutonium till over a million years.

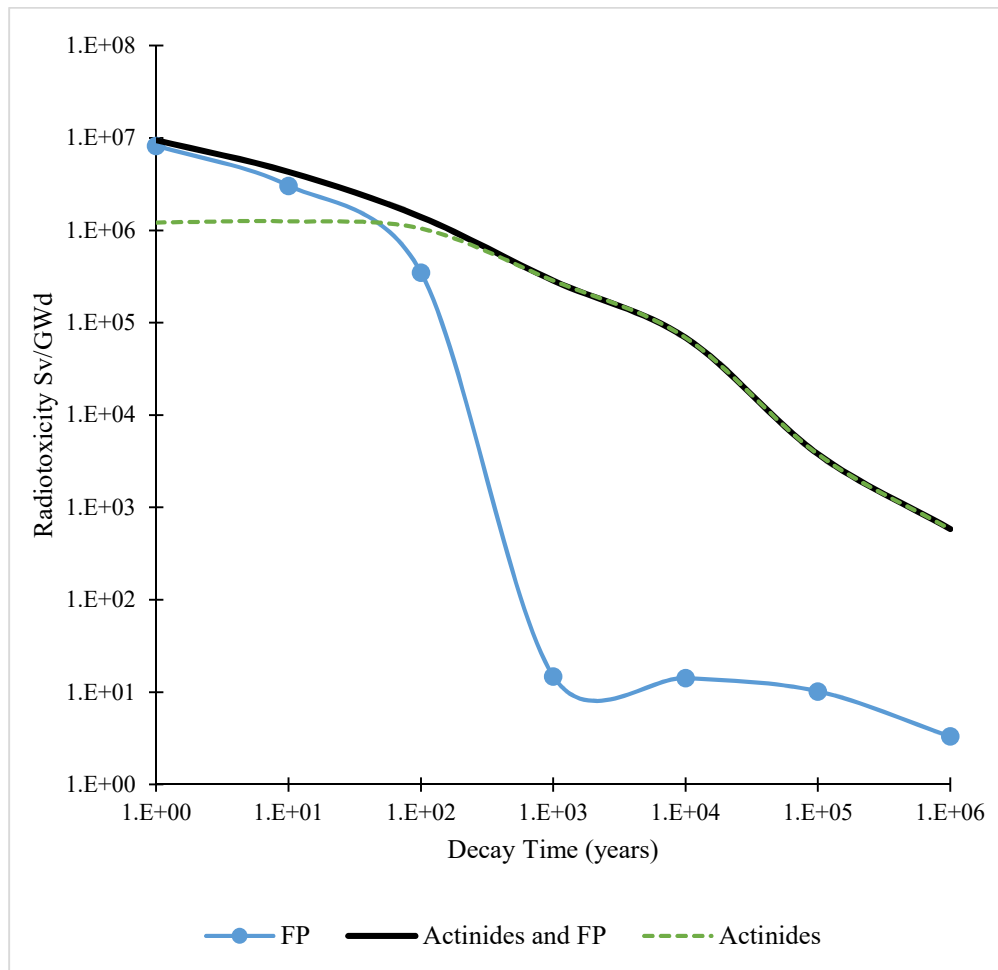


**Figure 5. 6 Ingestion Radiotoxicity from Fission Product and Actinide in EPR SNF**

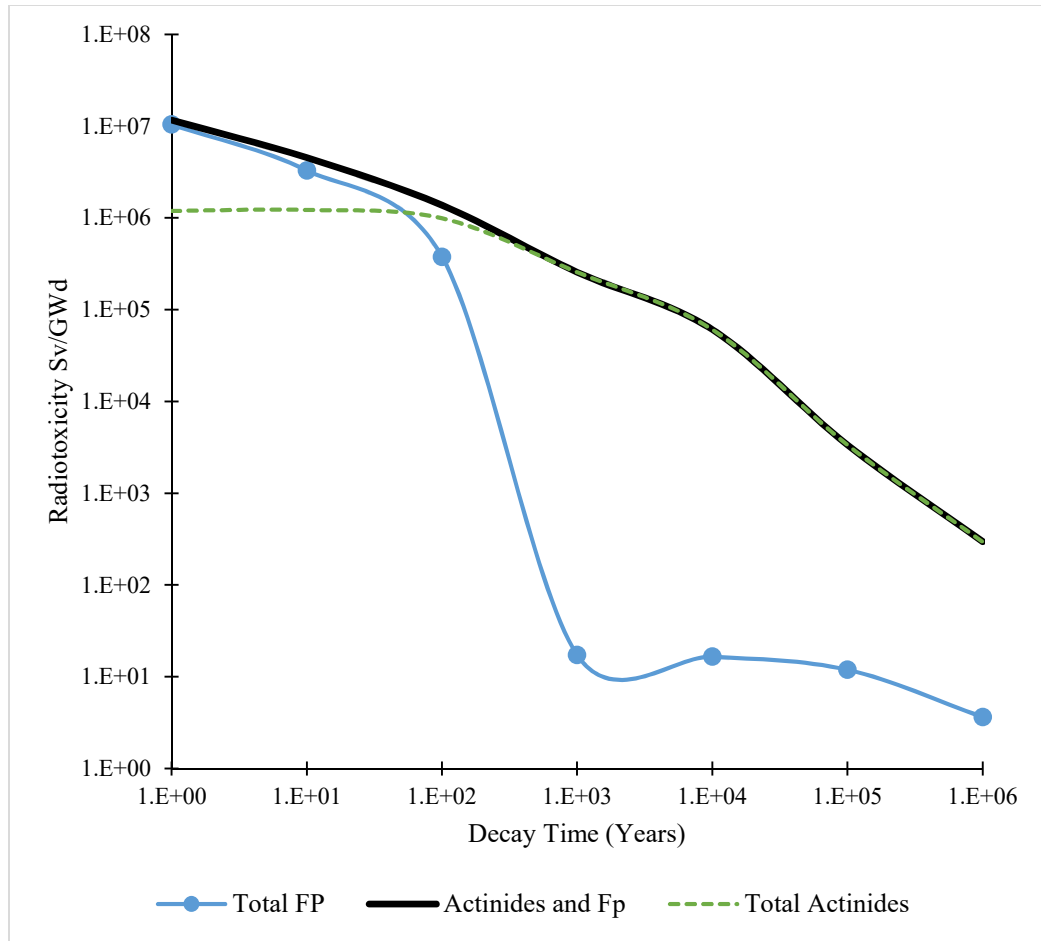


**Figure 5. 7 Ingestion Radiotoxicity from Fission Product & Actinide in HPR SNF**

### 5.6.2 Radiotoxicity by Ingestion from Actinides

Radiotoxicity by ingestion from actinides in the SNF for both EPR and HPR was determined and results shown below in Figure 5.8 and 5.9 below. It was observed that the plutonium isotopes has the highest effect on ingestion radiotoxicity for the EPR and HPR spent fuel till over a million years except for a few intervals between one hundred and a thousand years where americium isotope dominated the ingestion radiotoxicity. This is due to the buildup of Am-241 in the SNF by the  $\beta$ -decay of Pu-241.

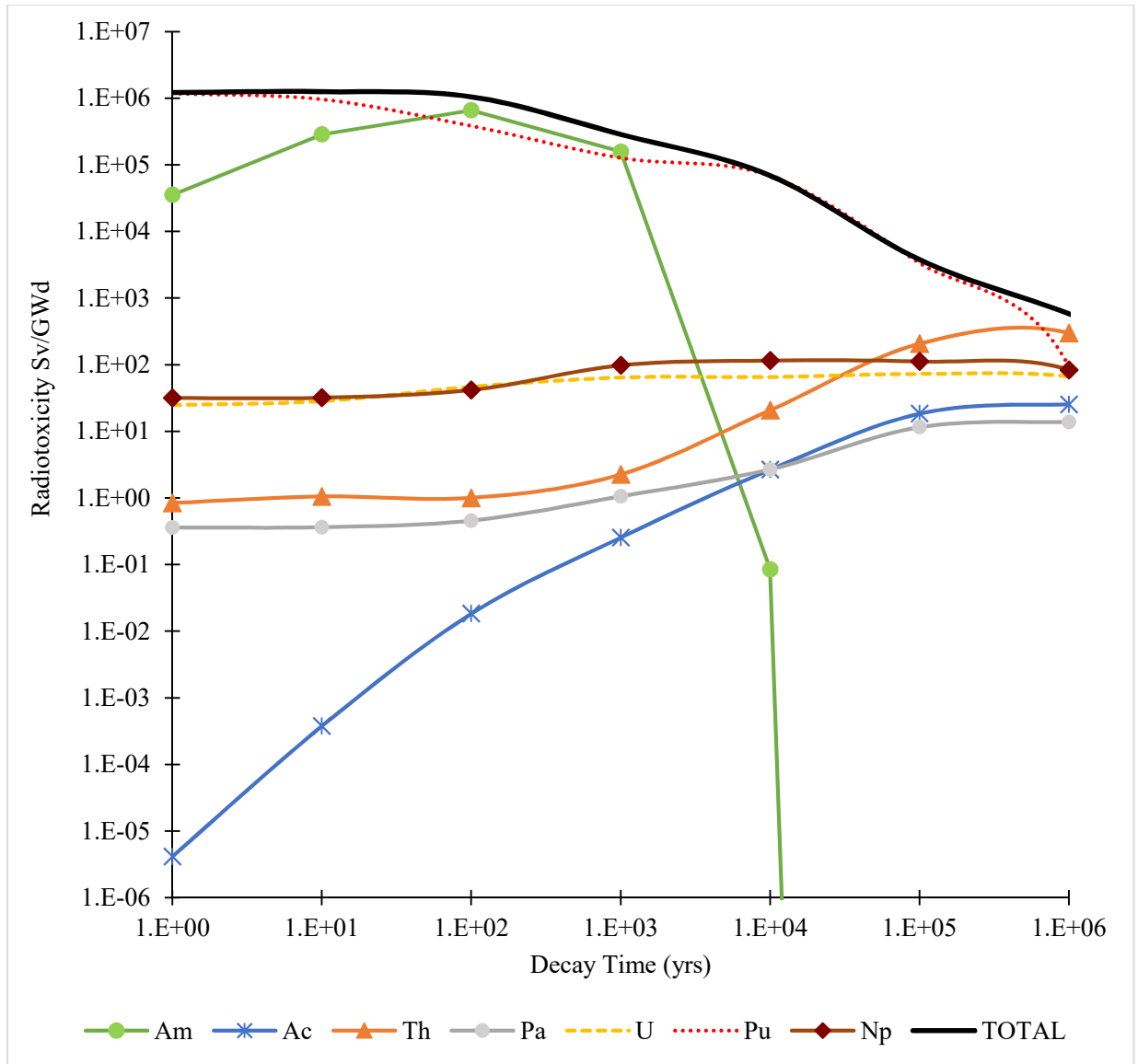


**Figure 5. 8 Ingestion Radiotoxicity by Actinides in EPR SNF**

Am-241 has a major effect on the ingestion radiotoxicity for thousands of years due to its half-life of about 432.2 years and high radioactivity and dose factor.



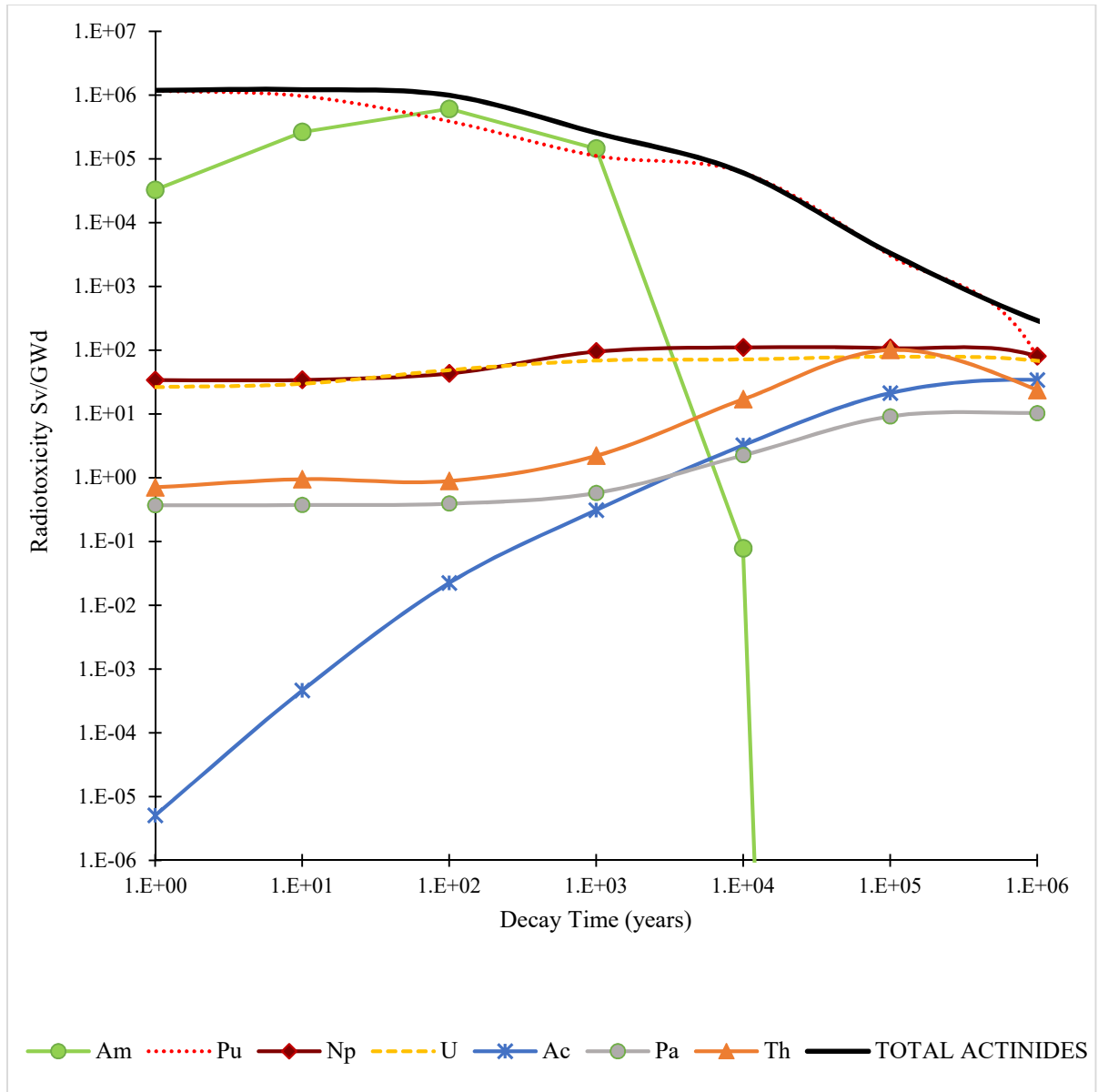


**Figure 5. 9 Radiotoxicity by Ingestion from Actinides in HPR SNF**

Thorium isotopes are also observed to build up in the fuels at 1,000years and above due primarily to the formation of Th-229 from the alpha decay of U-233 and also the formation of Th-230 also from alpha decay of U-238. They constited the major ingestion radiotoxicity impact from the thorium isotopes. They have half lifes of 7,340years and 75,380 years respectively and their impact on radiotoxicity is observed to persist over a million years.

Th-232 is also present in the SNF of both reactors and its radiotoxicity also buildup. The neutron irradiation and subsequent beta decay of Th-232 produces U-233 which is fissile. Th-232 can be extracted for its potential as nuclear fuel. Thorium isotopes impact on radiotoxicity is observed to be higher for the EPR SNF than for the HPR SNF. This is as a result of higher U-238 level in EPR SNF due to its lower enrichment level. Th-230 one of the major Thorium isotope contributor to radiotoxicity is formed from the alpha decay of U-238.

The build up of Neptunium isotopes is observed around ten thousand years in both SNF. Np-237 is the major isotope contributing to radiotoxicity from Neptunium isotopes that building up. It is formed due to the alpha decay of Am-241. It is observed that the Np-237 isotope starts building up around 10,000 years when Am-241 has decayed. This buildup is observed to be higher for the EPR SNF. This is due to the higher content of Am-241 in EPR SNF from which it is produced.

The impact of the uranium isotopes on radiotoxicity of EPR and HPR SNF is also observed to increase with storage time. This is due primarily to the further formation of U-235 from the alpha decay of Pu-239 and the formation of U-238 from alpha decay of Pu-242. Higher values were obtained for the EPR SNF. The major uranium isotope that has the highest radiotoxicity impact from the uranium isotopes is U-238. Its content is higher in EPR SNF than in HPR SNF due to the higher enrichment level of the HPR UOX fuel.

Actinium isotopes are also observed to build up for the SNF of the two reactors. This trend is due primarily to the build up of Ac-227 from the decay chain of Th-231, U-235, Np-239 and Pu-239. Its radiotoxicity impact is lowest as compared to the other actinides due to its

low activity, low dose factor and short halflife of 21.7years. Radiotoxicity impact of protactinium is also observed to build up with time due to the formation of Pa-231 from the decay chain of U-235. Pa-231 impact on radiotoxicity spreads beyond a million years due to its long halflife of 32,760years, and considerably high dose factor being an alpha emitter.

### 5.6.3 Plutonium isotopes Impact on the Ingestion Radiotoxicity

The individual Pu isotopes contribution to radiotoxicity was examined and result is shown in Figure 5.10 and Figure 5.11 for EPR and HPR respectively.

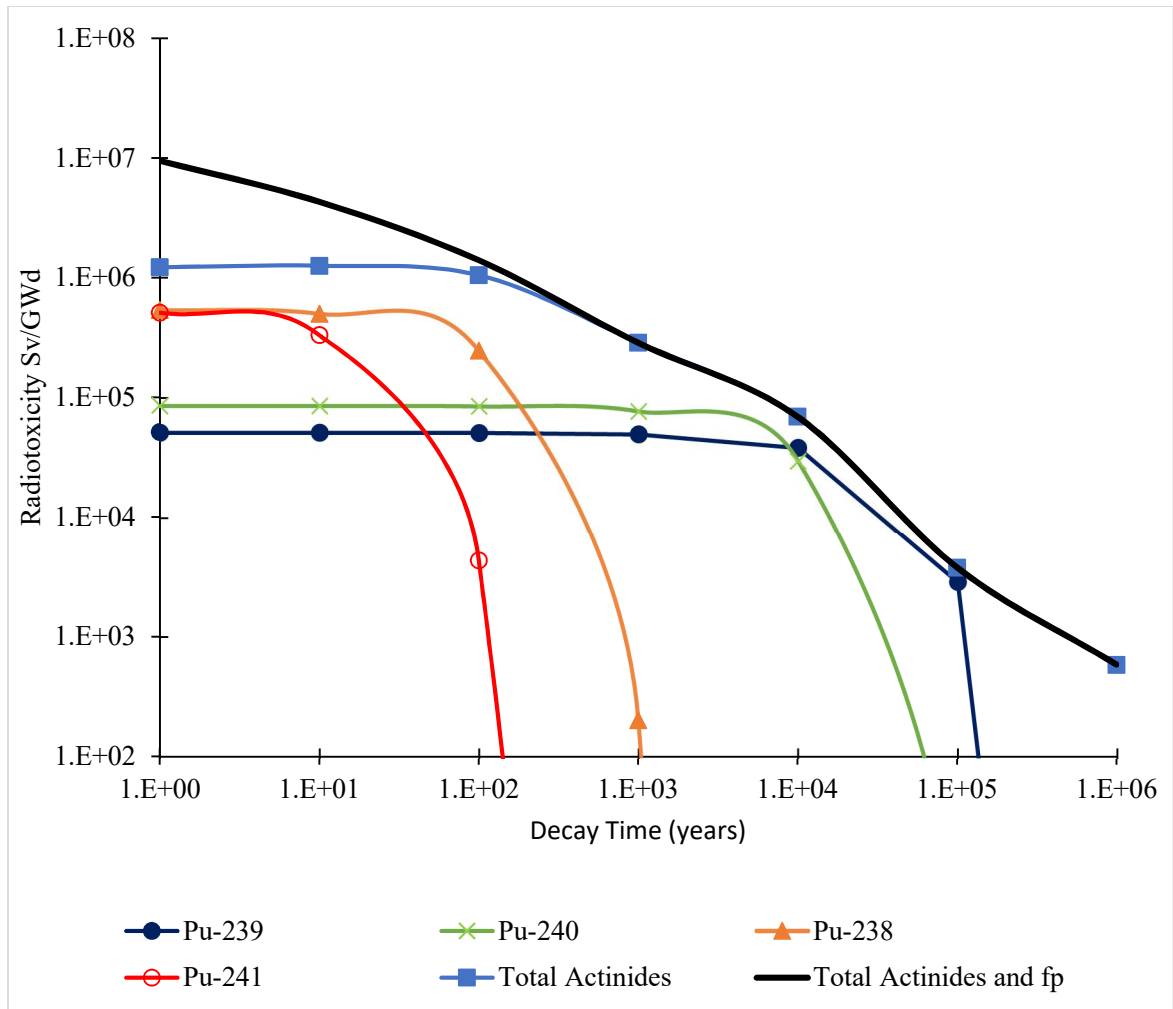
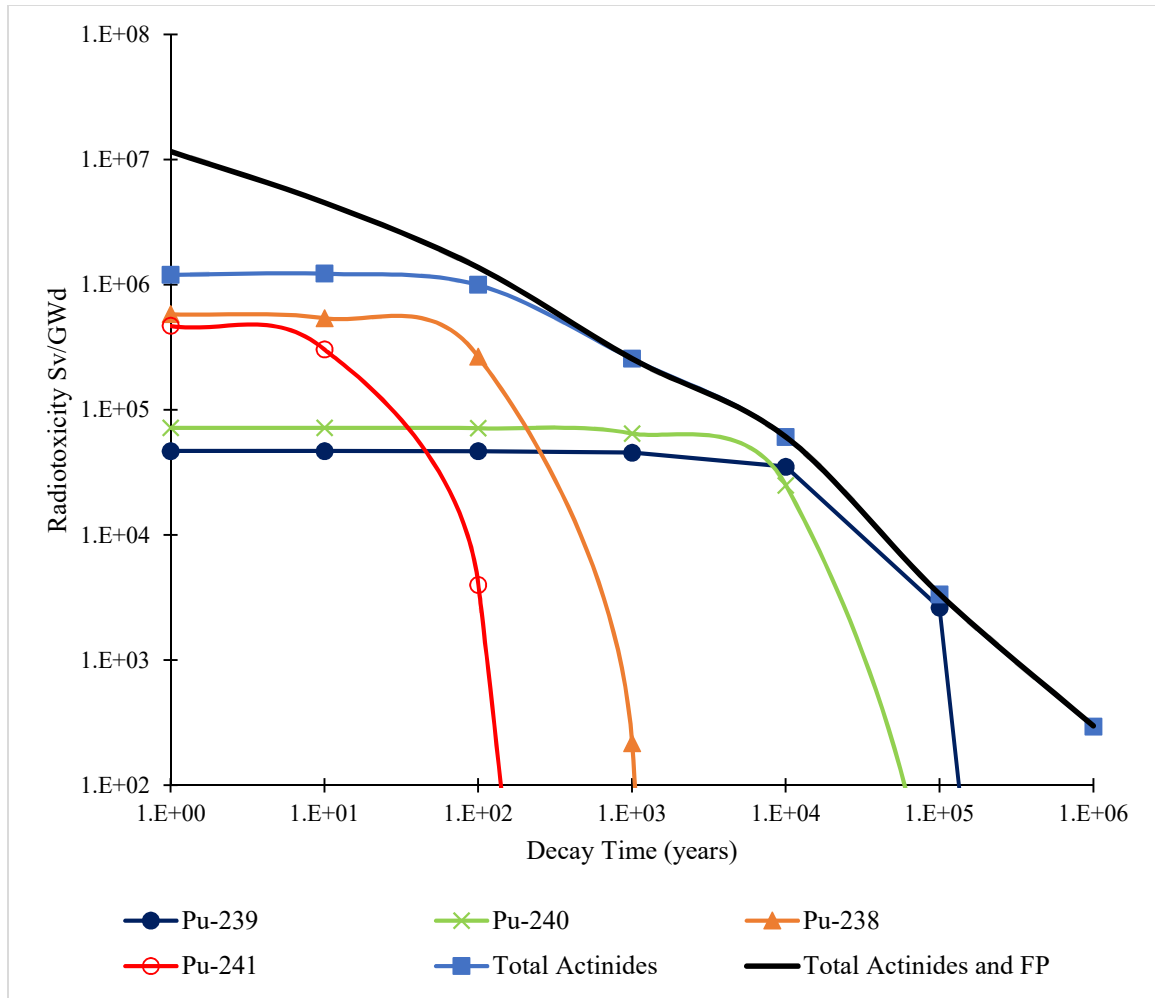


Figure 5. 10 Impact of Pu Isotopes on Radiotoxicity of EPR SNF



**Figure 5. 11 Impact of Pu Isotopes on Radiotoxicity of HPR SNF**

From Figure 5.10 and Figure 5.11 above, it is observed that the initial high radiotoxicity from plutonium is from the Pu-241 and Pu-238. Pu-241 and Pu-238 are both relatively short lived with half lives of 14.4 years and 88years respectively. It is observed that their impact on radiotoxicity only exist below 1,000years. Pu-241 is produced in the neutron capture reaction of U-235 without fission and also in the neutron capture of U-238. Its content is observed to be higher in the EPR SNF due to its lower enrichment level. Pu-241, a beta emitter decays into Am-241. It is less radiotoxic than the other alpha emitters of plutonium. Its high radiotoxicity value is a function of its initial high radioactivity though

its dose factor is lesser compared to the other plutonium isotopes. From the results, it is observed that Pu-238 is the main contributor to the radiotoxicity from the plutonium isotopes. This is because of its higher activity and dose factor as compared to Pu-241. Pu-238 is an alpha emitter. It is highly radioactive and it finds application as an energy source in remote spatial missions.

It is also observed that soon afterwards when Pu-241 and Pu-238 had decayed, the other isotopes of plutonium now dominates the radiotoxicity. The radiotoxicity trend of Pu-239 is also observed to span to the region of 100,000years before eventual decay. This is due to its radioactivity (its an alpha emitter), high dose factor and half life of 24,000 years. Pu-239 in itself is fissile but very little amount is produced in both reactors studied. However, Pu-239 needs to be properly stored away in a deep repository because it can be diverted to weapon if it gets to the wrong hands since it is known to generate fission and energy far more than that obtainable from U-235. Pu-239 decays by alpha emission into U-235. Also operating a fuel at higher burnup produces lesser radiotoxicity worry as is observed in the HPR SNF which produced lesser Pu-239 as compared to the EPR SNR. This is due to the higher burnup obtained from its UOX fuel. Pu-240 contribution to radiotoxicity is observed to be steady for over 10,000years. It is an alpha emitter thus it has a high dose factor with a long half live of 6,500years which is part of the reason for this observed trend in both reactor SNF. It is formed by the neutron capture reaction of Pu-239. It is a fertile isotope of plutonium as such, it does not undergo fission but piles up steadily with burnup. Allowing reactor fuel to stay longer in the reactor produces more of Pu-240 which reduces proliferation because it produces higher heat and spontaneously emmit neutrons.

#### **5.6.4 Fission Products Impact on Radiotoxicity**

The study was also conducted to check the fission product's contribution to the radiotoxicity of the SNF for both EPR and HPR. The results is shown below in Figure 5.12 and Figure 5.13. The result revealed that the initial high radiotoxiety from fission product is from the Cs-137 and Sr-90. However, the HPR SNF generated more of these two fission products. This is as a result of the initial enrichment of the HPR UOX fuel being higher than that of EPR. More fission took place for the HPR UOX fuel and more energy was produced from it for the one year operation period used. Cs-137 being one of the products of the fission of U-235 and other fissionable material in the fuel, has half life of 30.17 years and decays by beta emission to the meta stable isomer of Barium (Ba137) which has half life of about 113 seconds and spontaneously emits gamma rays. Cs-137 is highly radiotoxic as shown in the Figures but due to its short half life, it decays rapidly, shown by the large steep in its characteristic radiotoxicity curve. This implies that the SNF can be controllably stored for about 100years to eradicate the radiotoxicity of this fission product. The same applies for Sr-90 which has the highest radiotoxicity content from the fission products. Sr-90 is a beta emitter and decays into Yttrium90. It has high dose factor with a half life of 28.8 years and is only radiotoxic for a period of around 100 years after which its radiotoxicity reduced due to decay as shown by its steep characteristic curve in the figures 5.10 and 5.11 below. However Cs-137 and Sr-90 can be extracted from the SNF for their beneficial applications which will also reduce the radiotoxicity of the SNF. For example, they find application in industry for use in flow meters, thickness gauges and in well logging. They also find application in medicine in radiotherapy. After Cs-137 and Sr-90 has decayed, the radiotoxicity from fission products in the SNF is mainly from I-129 and Tc-99 as observed from the result. I-129 is formed in the fission of fissile isotope of

uranium and plutonium. It has half life of 15.7 million years. Its a low beta and gamma emitter and decays to Xe-129. Due to its very long half life, its radiotoxicity is observed in the results to span over a million years. It has no practical application but due to its long half life it can be used in radioactive dating. The highest radiotoxicity from the long lived fission products is from Tc-99. It decays by beta emission into Ru-99. It has a half life of 211,000 years and its radiotoxicity is observed to span above 100,000years before it decays as shown. Its metastable isomer has application in nuclear medicine in radiotherapy. It dominated the radiotoxicity of the SNF from fission products for around 1,000years till over 100,000years as observed from the result.

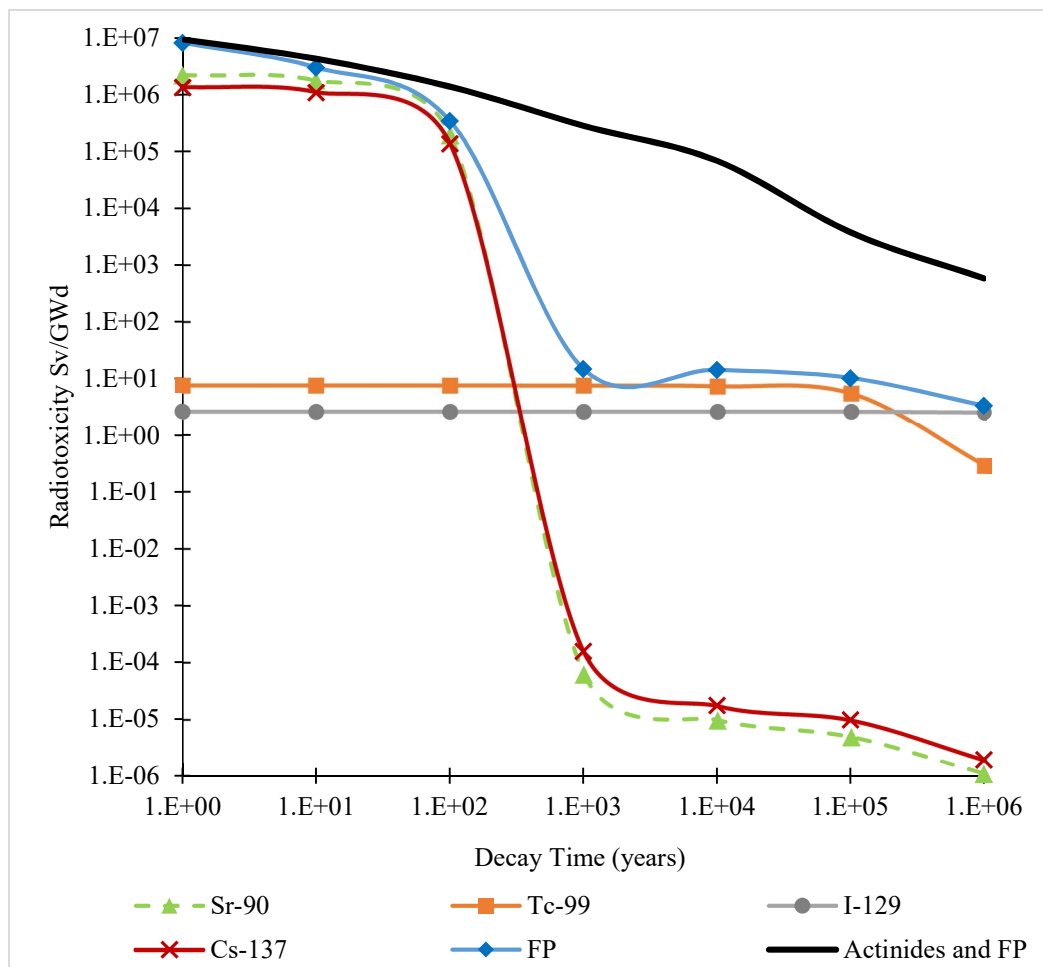
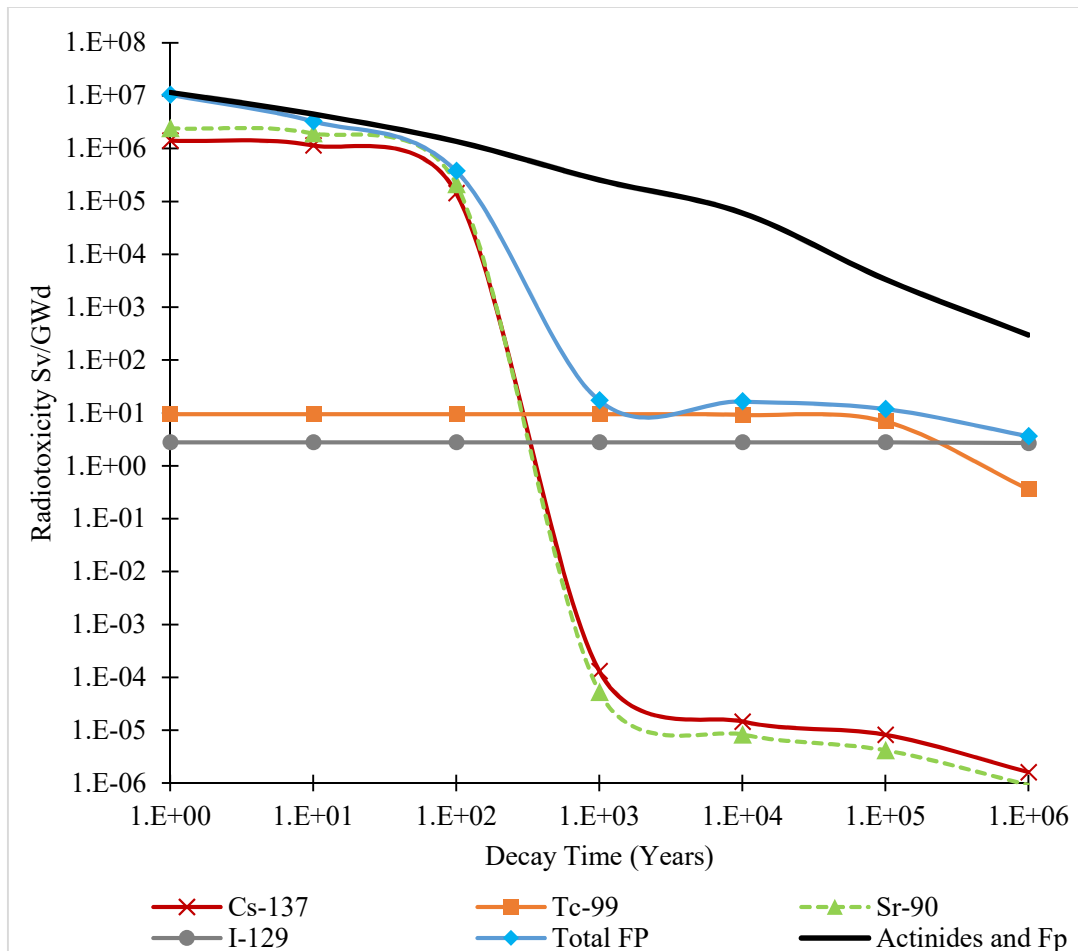


Figure 5. 12 Radiotoxicity by Ingestion from Fission Products in EPR SNF



**Figure 5. 13 Radiotoxicity by Ingestion from Fission Products in HPR**

**5.6.5 Comparison of the Ingestion Radiotoxicity with and without Pu and U**

A plot of the radiotoxicity by ingestion was made to compare the total radiotoxicity from the SNF to the radiotoxicity obtained after plutonium and uranium isotopes have been removed for both EPR and HPR, a process that can be achieved through chemical reprocessing. The result is as shown in Figures 5.14 and 5.15 below. It is observed that the total ingestion radiotoxicity from EPR SNF reduced drastically after about a thousand years. This is because when Pu has been removed, Am-241 did not build up in the SNF. All the other minor actinides comprising of the thorium, neptunium, protactinium and actinium isotopes that forms from the decay of the major actinides also did not build up

except for the ones that build up during reactor operation and they are observed to decay with time till a million years. Therefore, the radiotoxicity is predominantly from the fission products. And for about a thousand years, they have almost totally decayed. In the decay chain of Neptunium, some isotopes of thorium build up coupled with the ones already in the fuel. Pu-238 and Pu-239 also formed from the decay of Np-238 and Np-239 in the SNF. These and other radionuclides still present in the SNF also decay with time as shown till a million years.

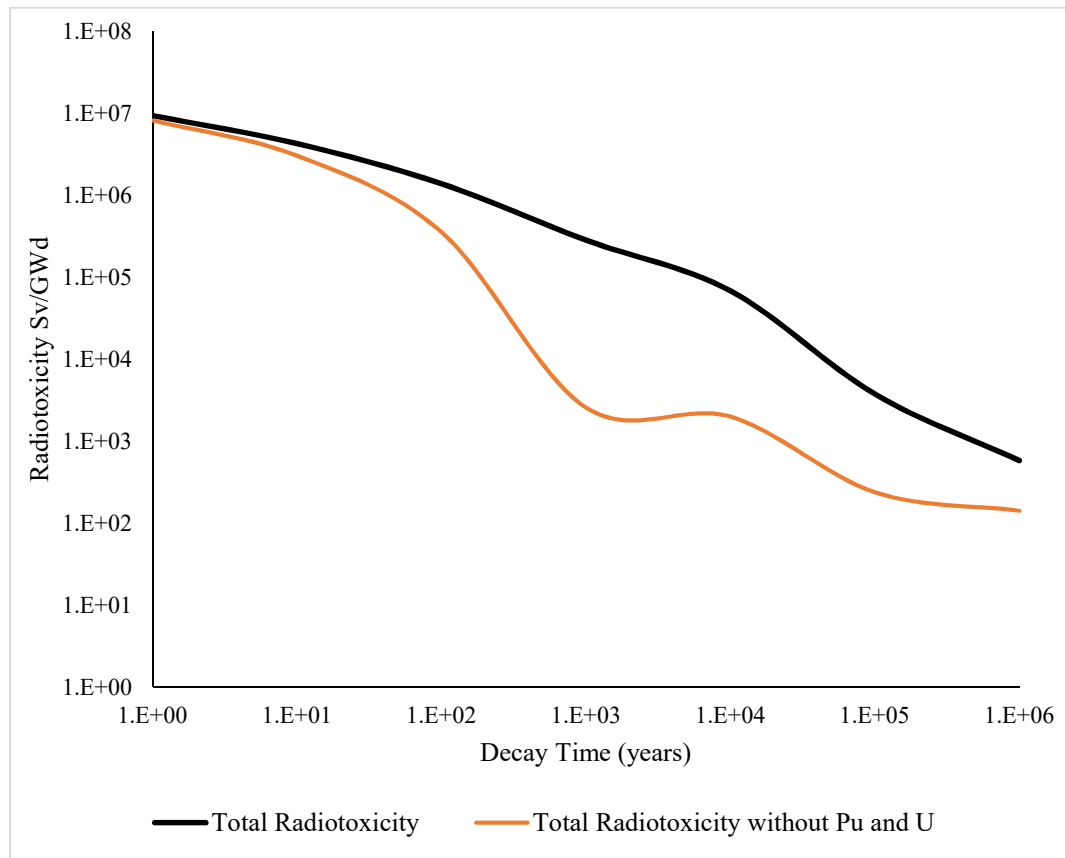


**Figure 5. 14 Radiotoxicity by Ingestion without Pu and Am Isotopes for EPR SNF**

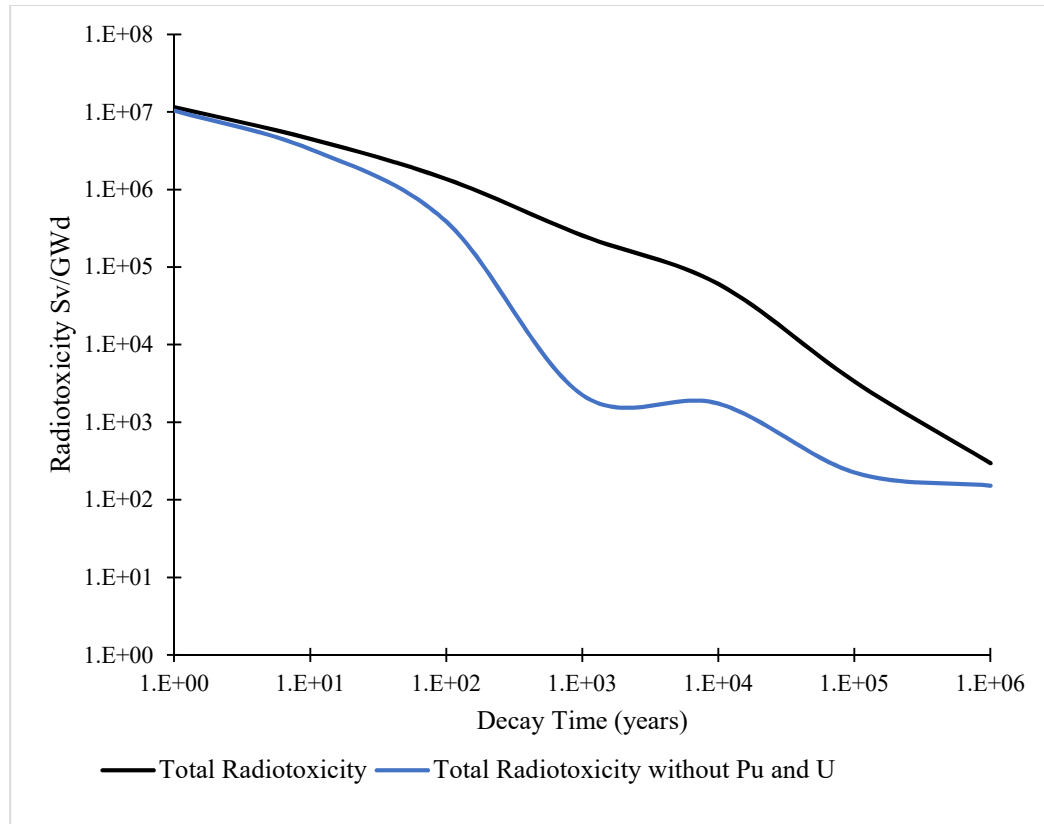


**Figure 5. 15 Radiotoxicity by Ingestion without Pu and U Isotopes for HPR SNF**

Sogbadji, et al., 2016, performed radiotoxicity study of UOX fuel of French EPR at burnup of 46GWd/t. The trend obtained in this study showed similarity with the results from Figure 2.2 in the literature review.

#### **5.6.6 Ingestion Radiotoxicity comparison for the EPR and HPR SNF**

A plot was made to compare the total ingestion radiotoxicity of the EPR and HPR SNF. The result is shown in Figure 5.16 below. It is observed that the initial radiotoxicity of the HPR surpasses that of the EPR below the first hundred years. This is as a result of the initial enrichment of the nuclear fuel of HPR which is higher than that of the EPR, thus producing more fission products, which constitute to this initial higher radiotoxicity value from HPR compared to EPR spent fuel. HPR fuel pins have an enrichment of 1.8% (minimum

enrichment for a fresh core), while the EPR fuel pins are modelled with an enrichment of 1.4% (minimum enrichment for a fresh core). However, at one hundred years and beyond till over a million years, EPR spent fuel dominate in radiotoxicity level.

From the design parameters, EPR fuel rods have a fuel diameter of 8.2mm while HPR has 8.192mm. Apart from that, the active height of EPR fuel rod is 4,199.99mm while that of HPR is 3,658mm. From this design parameters, EPR fuel rod have higher volume of fuel having higher concentration of U-238 than HPR fuel rod due to its lower enrichment level. Pu-239 is formed by the neutron capture process of U-238 followed by two beta decays. Pu-240 and Pu-241 are formed by further neutron capture processes. Pu-241 beta decays to Am-241. So, higher concentration of these isotopes is present in EPR spent nuclear fuel, thus making the EPR spent fuel to be more radiotoxic than HPR spent fuel in the long run.

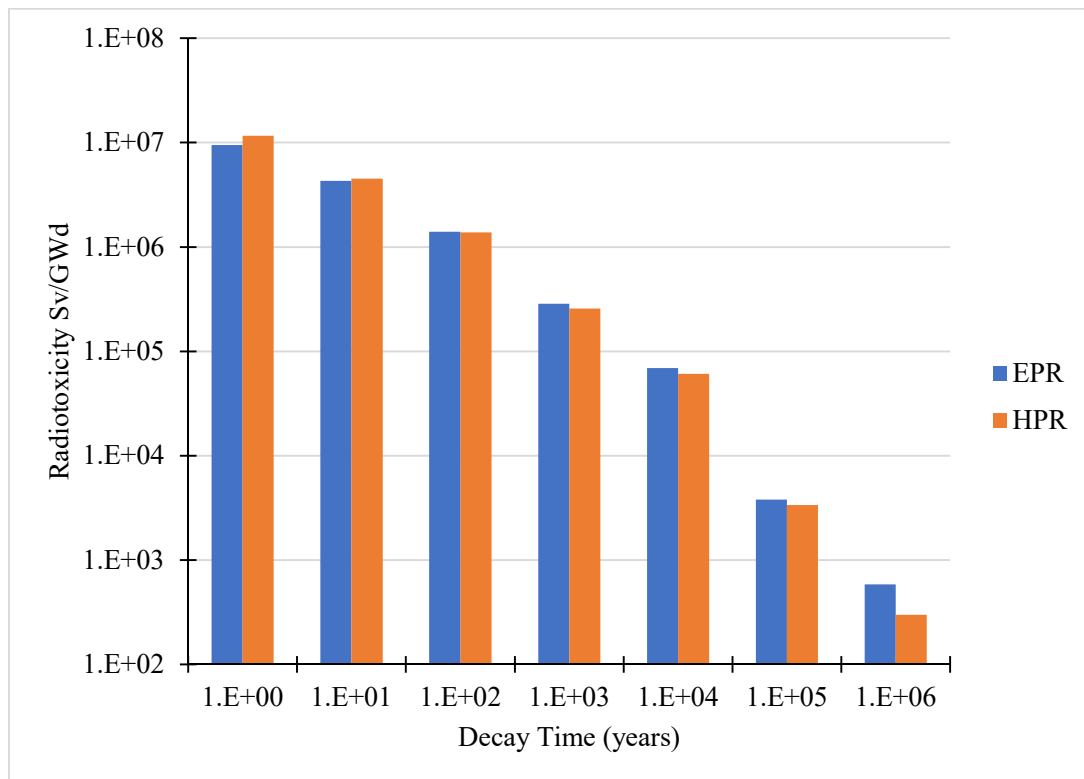


**Figure 5. 16 Comparison of Radiotoxicity by Ingestion For EPR and HPR SNF**

This chapter has presented results from the simulations and relevant discussions pertaining to the results provided.

The next chapter focuses on the conclusions drawn from the analysis of the results in this chapter. Appropriate recommendations based on the study is also given in the next chapter.

## CHAPTER SIX

### 6.0 Conclusion and Recommendation

#### 6.1 Conclusion

The MCNPX input deck for the EPR and HPR fuel assembly were successfully developed and simulation carried out. The fuel burnup calculation was done for each reactor at normal operating conditions.

Ingestion radiotoxicity calculation was determined for the SNF of the EPR and HPR up to a million years. The Radiotoxicity of SNF of the two reactors was compared. In the short term, the HPR SNF is more radiotoxic although it has a good fuel burnup. After a hundred years, the EPR SNF becomes more radiotoxic. This is due to its higher Pu isotope content. The highest radiotoxicity in the two reactor's SNF, in the first hundred years is from the fission products. According to the findings, the most radiotoxic being Cs-137 and Sr-90. Also, Pu isotopes constituted majority of the radiotoxicity from actinides in the SNF for both EPR and HPR.

After comparing the radiotoxicity of the SNF without the actinide that are major contributors to the radiotoxicity which includes mainly the Pu isotopes, a drastic drop in radiotoxicity was observed.

Based on the findings in this study, radiotoxicity of SNF of EPR and HPR reactors can be further reduced by reprocessing, which involves isolating the Pu and U isotopes from the SNF. This will go a long way in reducing the size of the repository and also increase the lifespan of the repository for EPR and HPR SNF. Furthermore, this will also decrease the

amount of Uranium ore mined and processed as fuel for the EPR and HPR type reactor technologies worldwide.

## **6.2 Recommendation**

With Ghana's decision to go nuclear for electricity generation, proper spent fuel management approach needs to be practiced to properly curtail the potential radiological hazard that could arise from SNF of the nuclear technology that will be adopted. This study has identified the radionuclides that could pose a threat to human health in the SNF of the reactors studied and can also serve as a guide for similar studies. However, this study did not take into consideration safety analysis and thermal hydraulic behavior, of the reactors considered. Therefore, It is my recommendation that further works in these areas be considered to further firm up the reactor of choice for the Ghana Nuclear Power Programme.

It was observed that the HPR SNF contains more Pu-240 than the EPR SNF. This is due to its higher burnup. High burnup fuels stay longer in the reactor and produces more of Pu-240. Pu-240 produces very high heat and spontaneously emits neutrons, making it unsuitable to be diverted to weapons use. Also operating a fuel at higher burnup produces lesser radiotoxicity worry as is observed in the HPR SNF which produced lesser Pu-239 as compared to the EPR SNR. Pu-239 needs to be properly stored away in a deep repository because it can be diverted to weapon if it gets to the wrong hands since it is known to generate fission and energy far more than that obtainable from U-235. Pu-239 decays by alpha emission into U-235, as such it is an alpha emitter and very radiotoxic. It is my recommendation that the HPR be further researched on and given due consideration by

the Ghana Nuclear Power Programme for its more environmental safety prospects of having a lesser radiotoxic SNF (in the long term) as compared to the EPR SNF.

It was also observed that Thorium exhibited high radiotoxicity for the SNF of the two reactors considered. It is my recommendation that the radiotoxicity of the Th-UOX fuel cycle being considered as fuel for future similar reactors be further investigated.

### References

1. Kalcheva, S., & Koonen, E. (2007). *MCNPX 2.6.C vs MCNPX & ORIGEN-S: State of the art for Reactor core Management*. Mol, Belgium: Belgium Nuclear Research Centre.
2. Aguilar, O., & Por, G. (1987). Monitoring Temperature Reactivity Coefficient by Noise Method in NPP at Full Power. *Annals of Nuclear Energy*, 1-6. Retrieved from [inis.iaea.org](http://inis.iaea.org)
3. Arafat, Y., Franceschini, F., Lahoda, E. J., Carelli, M., Wenner, M., Ferroni, P., . . . Petrovic, B. (2011). Radiotoxicity Characterization of HLW from Reprocessing of Uranium-Based and Thorium based fuel. Phoenix: WM.
4. AREVA. (2012). *US EPR Brochure, Paris-La Defense oedex France*. Framatone ANP.
5. Bergelson, B., Gerasimov, A., & Tikhomirov, G. (2005). Radiotoxicity and decay heat power of the spent nuclear fuel of VVER-1000 type reactors at long term storage. *Radiation Protection Dosimetry*, 115, 445–447. Retrieved from [doi:10.1093/rpd/nci211](https://doi.org/10.1093/rpd/nci211)
6. Boafo, E., Alhassan, E., & Akaho, E. (2014, July 19). Utilizing the burnup capability in MCNPX to perform depletion analysis. *Annals of Nuclear Energy*, 478–483. Retrieved from [www.elsevier.com/locate/anucene](http://www.elsevier.com/locate/anucene)
7. Brewer. (2009). *Criticality Calculations with MCNP5: A Primer*. Los Alamos National Laboratory.
8. Cao, Y., Gohar, Y., & Broeder, C. H. (2010). MCNPX Monte Carlo burnup simulations of the isotope correlation experiments in the NPP Obrigheim. *Annals of Nuclear Energy*, 1321–1328. Retrieved from [www.elsevier.com/locate/anucene](http://www.elsevier.com/locate/anucene)
9. Chang, G. S., & Ryskamp, J. M. (2000). Depletion analysis of mixed-oxide fuel pins in LWR. *Nuclear Technology*, 326-337.
10. CNNC. (2015). *HPR-1000 Technology*. China National Nuclear Corporation.
11. Csom, G., Feher, S., & Szieberth, M. (2001). Improved Method for P&T Strategy Selection by Long-Term Risk Evaluation of Nuclear Energy Systems. *Institute of Nuclear Techniques, Budapest University of Technology Hungary*. Retrieved from [www.iaea.org/inis/collection/public](http://www.iaea.org/inis/collection/public)

12. Eckerman, K. F., Wolbarst, A. B., & Richardson, A. C. (1987). *Limiting values of radionuclide intake and air concentration and dcf for ingestion, submersion and inhalation*. Oak Ridge, Tennessee: Oak Ridge National Laboratory.
13. Ennison, I., & Dzobo, M. (2018). Nuclear Power and Ghana's Future Electricity Generation. *IAEA Publication, IAEA-CN-164-1P01*.
14. European Nuclear Society. (2017). <https://www.euronuclear.org/info/encyclopedia/n/nuclear-power-plant-world-wide.htm>. Récupéré sur <https://www.euronuclear.org>.
15. Fensin, M. L. (2008). *Development of the MCNPX Depletion Capability, a Monte Carlo linked Depletion Method That Automates the Coupling between MCNPX and CINDER 90 for High Fidelity Burnup Calculations*. Florida: University of Florida.
16. Framatome ANP, Inc. (2005). *EPR Design Description*. Lynchburg, Virginia: Framatome ANP, Inc.
17. Francois, J., Guzmán, J., & Campo, C. (2009, May 22). Study of the radiotoxicity of actinides recycling in boiling water reactors fuel. *Nuclear Engineering and Design*, 1911–1915.
18. Glasstone. (1994). *Nuclear Reactor Engineering*. New York: Chapman & Hall.
19. Guanxing. (2012). <http://www.neimagazine.com/features/featurechinese-nuclear-fuel/>. Retrieved from <http://www.neimagazine.com>.
20. Hendricks. (2008). *MCNPX 2.6.0 Extensions*. Los Alamos, New Mexico: Los Alamos National Laboratory.
21. Joe, K., Jeon, Y.-S., Han, S.-H., Lee, C.-H., Ha, Y.-K., & Song, K. (2012, March 24). Determination of plutonium content in high burnup pressurized water reactor fuel samples and its use for isotope correlations for isotopic composition of plutonium. *Applied Radiation and Isotopes*, 931–936.
22. Kommalapati, R. R., Opoku, F. A., Du, H., & Huque, Z. (2016). *Nuclear Material Performance*. intech. Récupéré sur <http://www.intechopen.com/books/nuclear-material-performance>
23. Larmash, R. J. (2001). *Introduction to Nuclear Engineering*. New Jersey: Prentice Hall, Inc.

24. López, D., & Töre, C. (2007). *WWER fuel rod isotopics by MONTEBURNS 1.0 influence on the multiplication factor and comparison with the CB3 benchmark data*. Spain, Spain: SEA Shielding Engineering and Analysis.
25. Miller, W. F., & Lewis, E. E. (1993). *Computational methods of Neutron Transport*. Illinois: American Nuclear Society, INC.
26. Necas, V., Sebian, V., & Kocisk, K. (2005). Radiotoxicity and Risk Reduction of TRU Elements from Spent Fuel by Transmutation in the Light Water Reactor. (M. Haight, T. Chadwick, & P. Talou, Eds.) *American Institute of Physics*.
27. Pautz. (2005). Fuel assembly calculations using the method of discrete ordinates. *Nuclear Science and Engineering*(149(2)), pp. 197-210.
28. Pelowitz. (2011). *MCNPX user's manual version 2.7.0*. Los Alamos National Laboratory.
29. Salome, J., Cardoso, F., Velasquez, C., Pereira, F., Barros, G., & Pereira, C. (2016). VHTR, ADS and PWR Spent Nuclear Fuel Analysis. *Procedia Chemistry*, 255 – 262.
30. Schwarz. (2011). *MCNP/MCNPX Visual Editor Computer code manual*.
31. Sogbadji, R., David, S., Akaho, E., & Nyarko, B. (2016, December). Neutronic Study of the Mono-Recycling of Americium In PWR. *Journal of Environmental Research, Engineering and Management, Vol. 72 / No. 3 / 2016*, 18-26. Retrieved from <http://dx.doi.org/10.5755/j01.arem.72.3.12790>
32. Staff, Los Alamos National Laboratory. (2008). *MCNP - A General Monte Carlo NParticle Transport Code, Version 5*. Los Alamos, NM : Los Alamos National Laboratory,.
33. Waata, C. L. (2006). Coupled Neutronics / Thermal-Hydraulics analysis of a High-Performance Light-Water Reactor Fuel Assembly,. *Germany: In: FZKA 7233, Forschungszentrum Karlsruhe*.
34. wikipedia, the free encyclopedia. (2018). [https://en.wikipedia.org/wiki/Nuclear\\_energy\\_in\\_South\\_Africa](https://en.wikipedia.org/wiki/Nuclear_energy_in_South_Africa). Récupéré sur <https://en.wikipedia.org>.
35. Wilson. (2008). *A Manual for CINDER'90 Version 07.4 Codes and Data*. Los Alamos: Los Alamos National Laboratory.

36. World Nuclear Association. (2017). *<http://www.world-nuclear.org/information-library/nuclear-fuel-cycle/introduction/nuclear-fuel-cycle-overview.aspx>*. Retrieved from <http://www.world-nuclear.org>.
37. *www.modernghana.com*. (2008). Retrieved from <http://www.modernghana.com/news152677/1/ghana-goes-nuclear-2018.html>: